Advanced Fusion Fuel Cycles and Fusion Reaction Kinetics - Preliminary Proposal

G.W. Shuy

December 1979

UWFDM-335

FUSION TECHNOLOGY INSTITUTE

UNIVERSITY OF WISCONSIN

MADISON WISCONSIN

Advanced Fusion Fuel Cycles and Fusion Reaction Kinetics - Preliminary Proposal

G.W. Shuy

Fusion Technology Institute
University of Wisconsin
1500 Engineering Drive
Madison, WI 53706

http://fti.neep.wisc.edu

December 1979

UWFDM-335

Advanced Fusion Fuel Cycles and Fusion Reaction Kinetics

Geoffrey W. Shuy

Preliminary Proposal

Nuclear Engineering Department
University of Wisconsin-Madison

UWFDM-335

Dec. 1979

Advanced Fusion Fuel Cycles

and

Fusion Reaction Kinetics

Table of Contents

I. Introduction

A large number of light elements will fuse if the temperature of the mixture is sufficiently high. The potential fusion fuel cycles can be classified as deuterium based, proton based and helium 3-based. The deuterium based fuel cycles include d-t, d-d, d-^{3}He and d-^{6}Li. The proton based fuel cycles include p-^{11}B and p-^{6}Li.

Fusion devices utilizing the d-t-Li cycle will certainly be the first to demonstrate energy breakeven and also very likely will be the first cycle for commercial fusion reactors. Nevertheless, fusion reactors with tritium fuel should be viewed as an intermediate step in fusion power development. The ultimate goal is to achieve a reactor based on either hydrogen or deuterium to insure both an inexhaustible fuel supply and systems with minimum radioactivity. To preserve this potential, it is essential to maintain efforts to develop advanced fuel cycle fusion power based on d-d, d-^{3}He, d-^{6}Li or proton based cycles such as p-^{11}B and p-^{6}Li. Minimizing the plasma deuterium content is a key to a minimum neutron producing reactor.

The potential advantages of a proton based fusion reactor are summarized in Table 1. First, both fuels in p-^{11}B or p-^{6}Li are abundant. Secondly, there is little gaseous radioactivity and no need to breed tritium. The elimination of tritium breeding and fueling minimizes problems of tritium management and eliminates in many cases the need for an intermediate loop in the power cycle. Thirdly, the neutron level is so low that bulk radiation damage to materials is not an issue. This impacts favorably

Table 1

Potential Advantages of Proton-Based Fusion Reactors

1. Fuels are essentially inexhaustible.
2. No gaseous radioactivity.
3. No fuel breeding requirement.
4. Simple blanket design - blanket is now just a first wall.
5. No radiation damage to structural materials.
6. Safety aspects more similar to coal plants than to nuclear power.
7. Improved system maintainability and thus, potentially, improved reliability and availability.
8. Very low levels of induced radioactivity.
9. Potentially low environmental impact on air pollution, mining, and long term solid waste disposal.
10. Potential for good system economics.
    - A. Balance of plant costs should be similar to coal plant. Nuclear oriented subsystems are minimized.
    - B. Fuel costs will be less than for nuclear.
    - C. Fusion island costs can be greater than for nuclear.
    - D. No intermediate loop required for safety.

on reactor design by permitting improved maintainability, availability and reliability. Some neutron induced radioactivity will result from deuteron reactions but this depends on branching ratios. Together with the absence of gaseous radioactivity, this low radioactivity and tritium level provides particular environmental advantages that will affect costs, licensing and siting. Fourthly, although the plasma power density is likely to be lower than in a d-t reactor with the same β value, the size limitations imposed by the neutron wall loading in d-t systems do not in any case permit one to take full advantage of very high β. With a minimum neutron advanced fuel cycle, magnets can be closer to the reaction chamber to offset the need for somewhat higher fields. Since the energy is released primarily as charged particles and electromagnetic radiation, the blanket is no more than the first wall itself. Fifthly, the bremsstrahlung radiation associated with a burning temperature of 200-300 keV is characterized by attenuation lengths on the order of .1-1. mm for either a low Z or medium Z material such as stainless steel. Since the first wall thickness is also on this order, the heat load has been converted to a volumetric heat load. By doping the first wall coolant with high Z material, the heat transfer problem is then simplified. In short, a proton based fusion reactor would be the fusion analog of a coal fired boiler. Cost advantages can be gained by eliminating systems such as intermediate heat exchangers, tritium extraction, tritium cleanup, radioactive waste control and remote handling. Potential environmental advantages can minimize licensing and siting issues. These cost savings can be used to a degree to offset disadvantages such as lower plasma power density.

The proper determination of the potential of an advanced fuel cycle requires a study of fusion reaction kinetics, including subtle effects like fast fusion, nuclear elastic and inelastic scattering, Doppler broadening of the energy distribution of reaction products, and the fraction of slowing down energy given separately to the ions and electrons.

There are two new effects in the analysis of advanced fuel cycles which have been investigated and found to increase the reactivity of the cycles, to alter energy balance calculations and to affect predicted Q values or ignition conditions. The first effect is the propagation in the cycles such as p-^{6}Li. ^{3}He, the energetic p+^{6}Li reaction product, reacts with ^{6}Li and produces an energetic proton before slowing down; these protons can undergo fast fusion again and propagate the reaction further. The second effect is the enhanced fast fusion reactivity due to nuclear elastic scattering. Nuclear elastic scattering of the energetic fusion products with the background fuel ions produces additional energetic particles which can undergo fast fusion and further propagate the reaction.

The proton-deuterium nuclear elastic scattering cross section is shown in Fig. 1 as a function of proton energy. The coulomb scattering cross section has been subtracted prior to plotting the result. The nuclear elastic scattering cross section is typically 1 barn or greater when the incident energy is in the range 1 to 15 MeV.

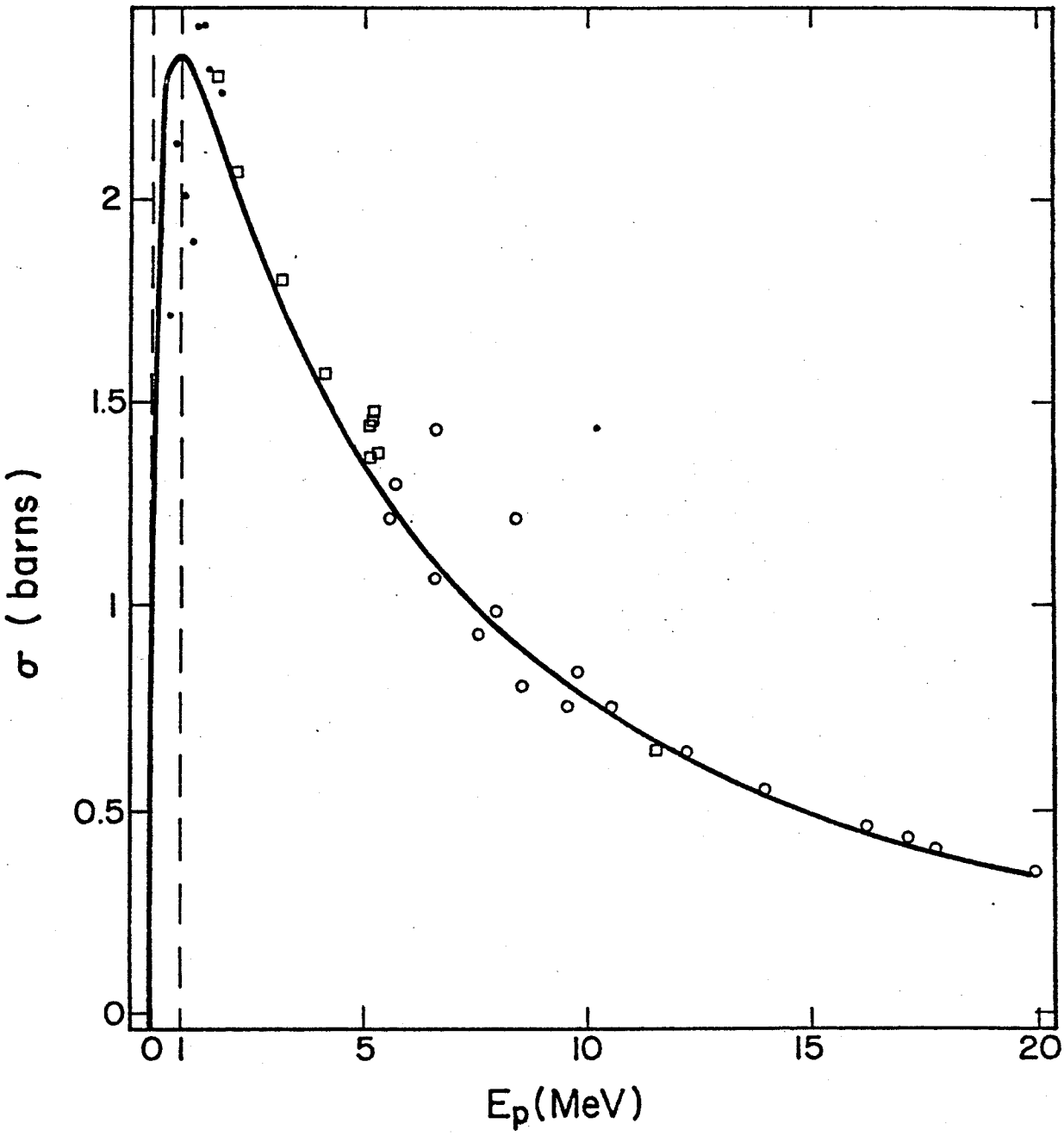

Fig. 1 The proton-deuterium nuclear elastic scattering cross section.

The average energy transfer per collision is large. For example, counting only collisions which transfer 1 MeV or more, a 3 MeV proton in a deuterium plasma with a 75 keV ion temperature is found to transfer ~ 30% of its energy to the energetic deuterons when the electron temperature is 60 keV. This fraction increases to ~ 50% when T_e is 100 keV. The fast fuel ions produced from the process undergo fusion while slowing down, thereby enhancing the reactivity and the propagation of the reaction. Figs. 2 and 3 show the fraction of energy transferred from fast alphas and fast protons to produce energetic deuterons with an energy greater than 1 MeV. The effect for alphas at 3 to 4 MeV is smaller than for protons at either 3 MeV or 14.5 MeV because of the larger coulomb cross section for alphas.

The catalyzed d-d fuel cycle can be used to elaborate on the role of nuclear elastic scattering and propagation enhancement. The major reactions for this cycle are:

$$d + d \begin{cases} \rightarrow n\ (2.45\ \text{MeV}) + {}^{3}\bar{\text{He}}\ (.87\ \text{MeV}) & (1) \\ \rightarrow \bar{p}\ (3.01\ \text{MeV}) + \bar{t}\ (1.\ \text{MeV}) & (2) \end{cases}$$

$$d + t \rightarrow n\ (14.06\ \text{MeV}) + \bar{\alpha}\ (3.5\ \text{MeV}) \quad (3)$$

$$d + {}^{3}\text{He} \rightarrow \bar{\bar{p}}\ (14.68\ \text{MeV}) + \bar{\alpha}\ (3.67\ \text{MeV}) \quad (4)$$

The overbars denotes fast charged particles. Nuclear elastic events such as

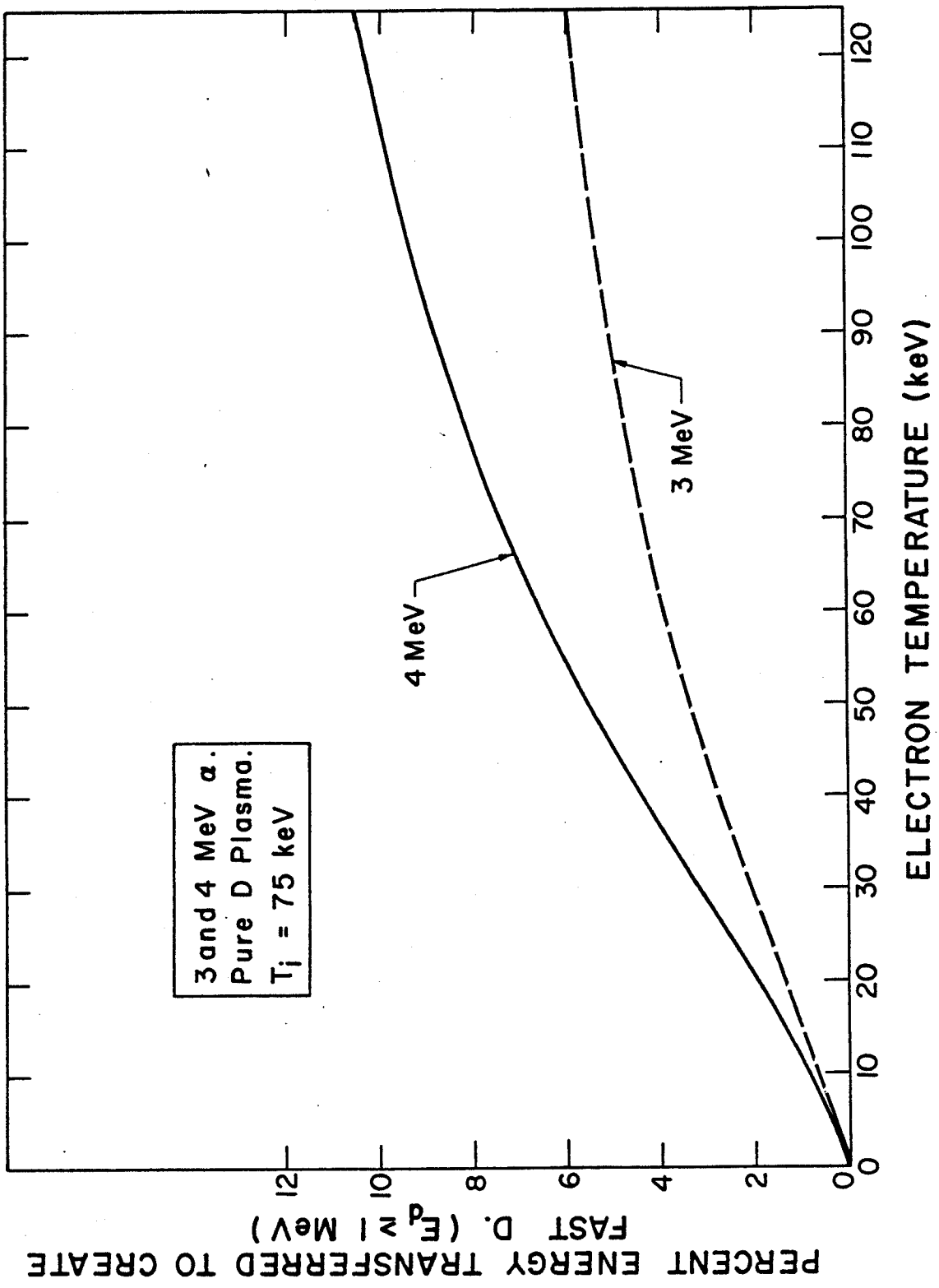
PERCENT ENERGY TRANSFERRED TO CREATE FAST D. ($E_d \geq 1$ MeV)
0
2
4
6
8
10
12
0
10
20
30
40
50
60
70
80
90
100
110
120
ELECTRON TEMPERATURE (keV)
4 MeV
3 MeV
3 and 4 MeV α.
Pure D Plasma.
T_i = 75 keV

Fig. 2

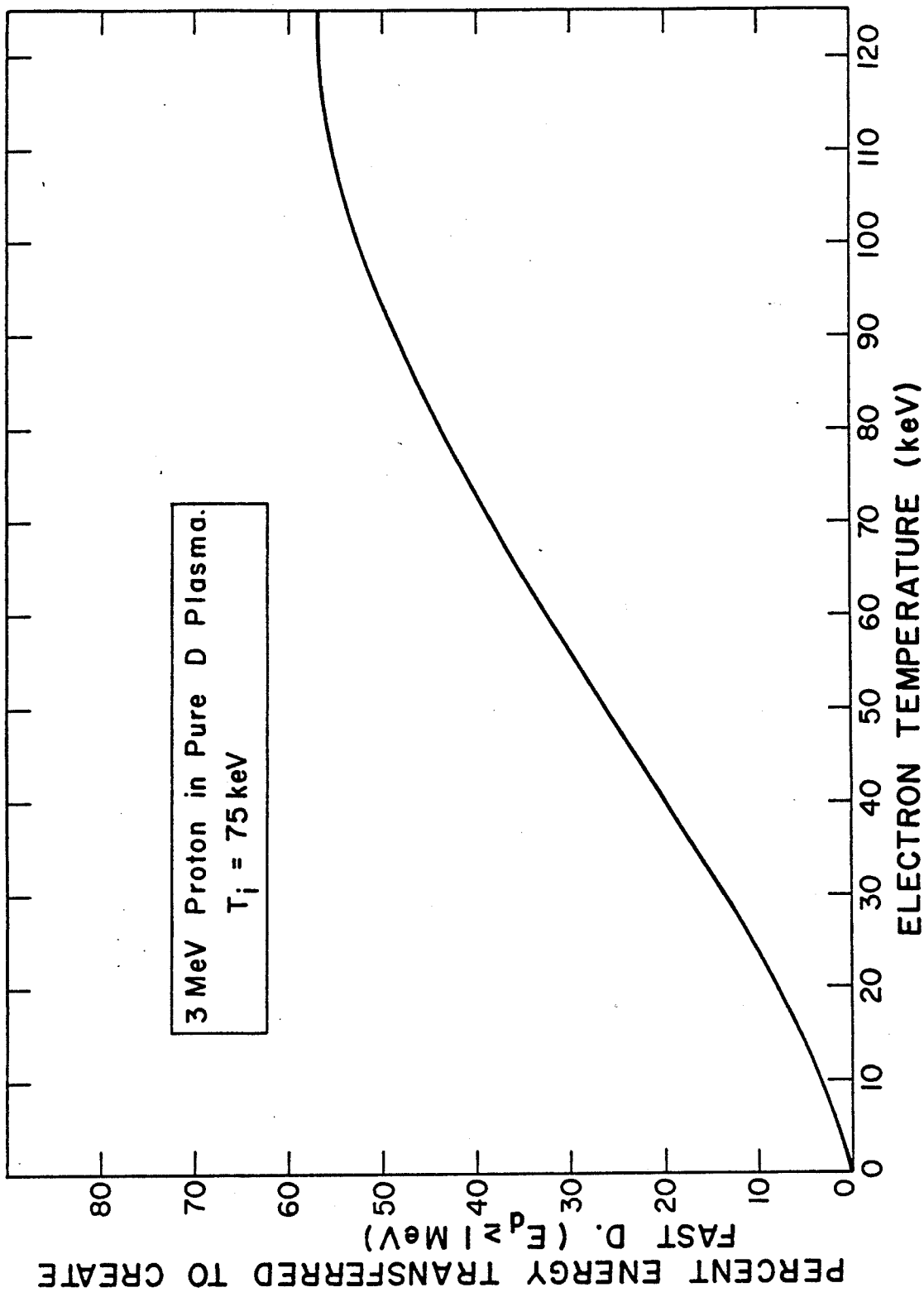
3 MeV Proton in Pure D Plasma.
T_i = 75 keV
PERCENT ENERGY TRANSFERRED TO CREATE FAST D. ($E_d \geq 1$ MeV)
ELECTRON TEMPERATURE (keV)
0
10
20
30
40
50
60
70
80
90
100
110
120

Fig. 3a

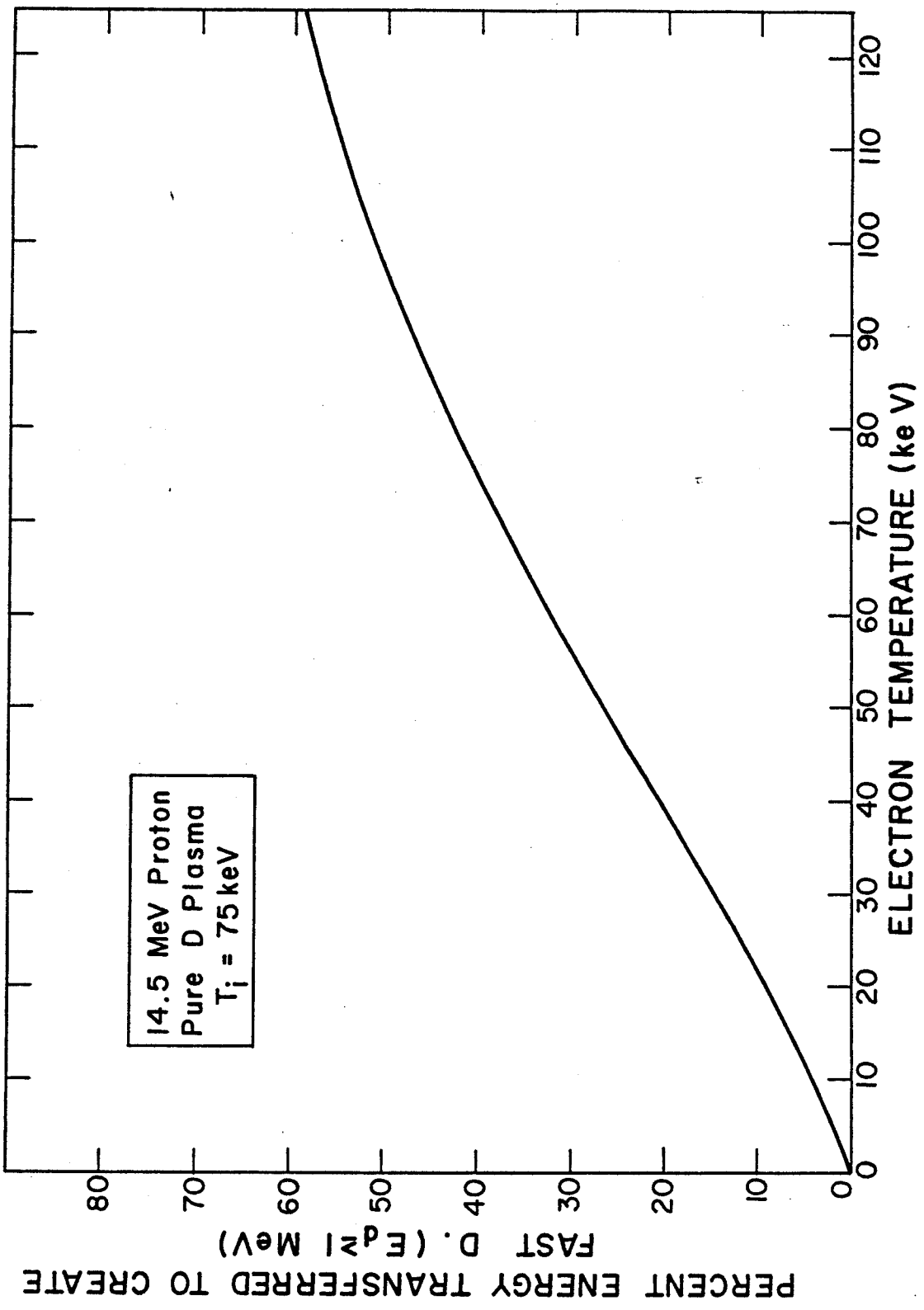
14.5 MeV Proton
Pure D Plasma
T_i = 75 keV
PERCENT ENERGY TRANSFERRED TO CREATE
FAST D. ($E_d \geq 1$ MeV)
ELECTRON TEMPERATURE (ke V)
0
10
20
30
40
50
60
70
80
90
100
110
120

Fig. 3b

$$\bar{p} + d \rightarrow p + \bar{d} \qquad (5)$$

$$\bar{\alpha} + d \rightarrow \alpha + \bar{d} \qquad (6)$$

$$\vdots$$

promote fast deuterons from the background Maxwellian distribution. A few of the propagating sequences in this cycle are:

$$\left\{\begin{array}{l} d + d \rightarrow \bar{p} + \bar{t} \\ \bar{p} + d \rightarrow \bar{d} + p \\ \bar{d} + d \rightarrow \bar{p} + \bar{t} \end{array}\right\} \qquad (7)$$

$$\vdots$$

$$\left\{\begin{array}{l} d + d \rightarrow {}^{3}\bar{H}e + n \\ {}^{3}\bar{H}e + d \rightarrow \bar{\bar{p}} + \bar{\alpha} \\ \bar{\bar{p}} + d \rightarrow \bar{d} + p \\ \bar{d} + d \rightarrow {}^{3}\bar{H}e + n \end{array}\right\} \qquad (8)$$

$$\vdots$$

$$\left\{\begin{array}{l} d + d \rightarrow \bar{t} + \bar{p} \\ \bar{t} + d \rightarrow \bar{\alpha} + n \\ \bar{\alpha} + d \rightarrow \bar{d} + \alpha \\ \bar{d} + d \rightarrow \bar{t} + \bar{p} \end{array}\right\} \qquad (9)$$

$$\vdots$$

$$\left\{\begin{array}{l} d + d \rightarrow {}^{3}\bar{H}e + n \\ {}^{3}\bar{H}e + d \rightarrow \bar{\alpha} + \bar{\bar{p}} \\ \bar{\alpha} + d \rightarrow \bar{d} + \alpha \\ \bar{d} + d \rightarrow {}^{3}\bar{H}e + n \end{array}\right\} \qquad (10)$$

$$\vdots$$

As an example, the propagating sequence indicated in set (7) produces fast protons. The fast proton promotes the deuterons out of the thermal bath; the energetic deuteron then reacts before slowing down, producing a fast proton, and so on.

The inclusion of these effects increases the reactivity of the catalyzed d-d cycle at T_i = 75 keV by 25% when T_e is 50 keV and by 75% when T_e is 100 keV. The results are shown in Fig. 4. These increases are measured relative to a standard calculation in which nuclear elastic scattering and propagating reactions are neglected.

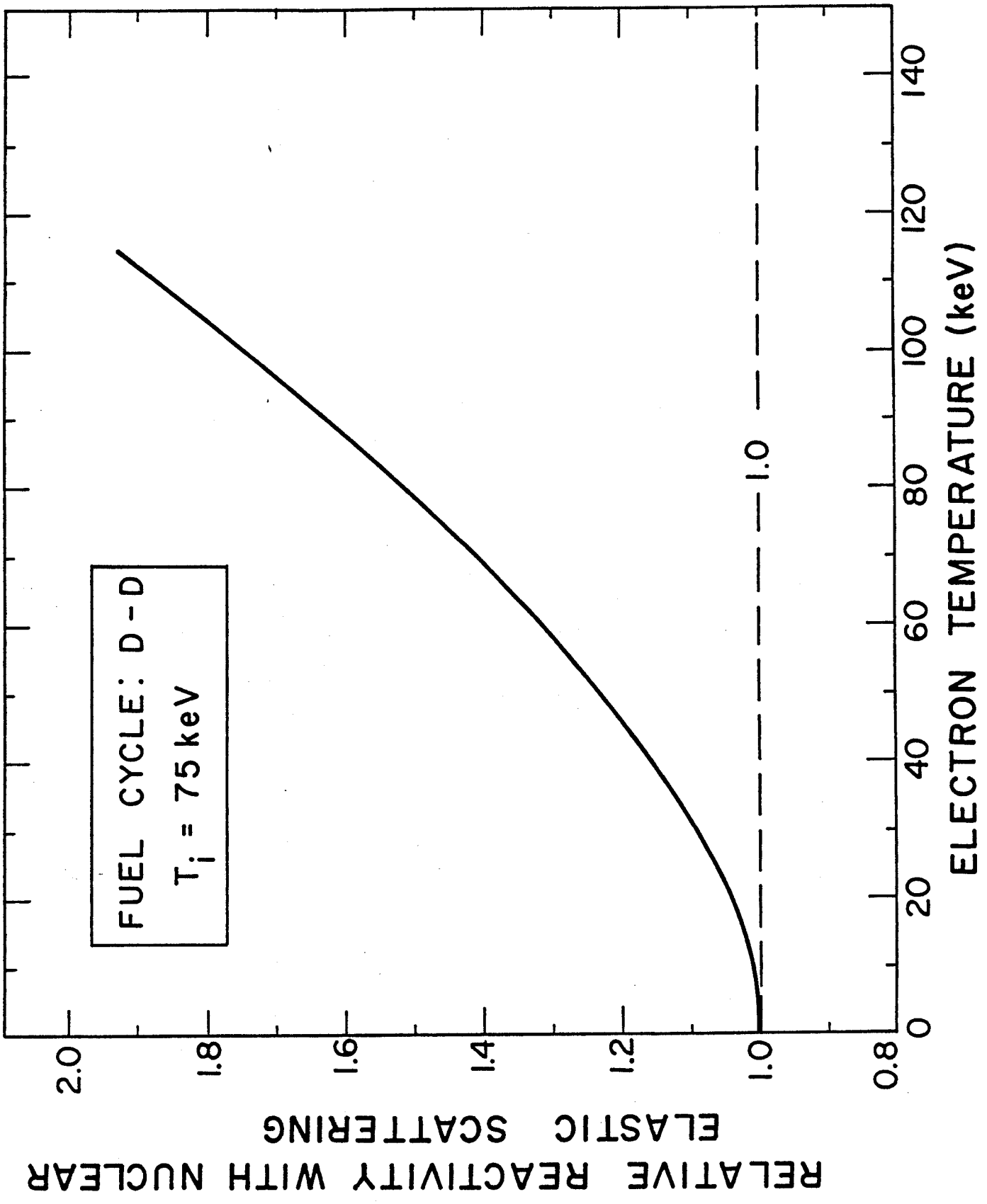
RELATIVE REACTIVITY WITH NUCLEAR ELASTIC SCATTERING
2.0
1.8
1.6
1.4
1.2
1.0
0.8
FUEL CYCLE: D-D
T_i = 75 keV
1.0
0
20
40
60
80
100
120
140
ELECTRON TEMPERATURE (keV)

Fig. 4

A nuclear knock-on event also alters the fraction of energy given to electrons and ions by energetic fusion products. The energy transferred to electrons by various fast particles (a 4 MeV alpha, a 3 MeV proton, and a 14.5 MeV proton) is shown in Figs. 5, 6 and 7 as a function of electron temperature. The dashed curve in each figure is the fraction of the initial energy received by electrons when only the coulomb interaction is assumed. The dash-dot curves in each figure give the analogous result when both coulomb and nuclear elastic scattering are included. Finally, the solid curve properly includes the effect of fast ion production by nuclear scattering and the subsequent slowing down of those ions with background ions and electrons. The background plasma in all cases is composed of electrons and deuterium ions. The ion temperature is fixed at 75 keV. While the inclusion of the nuclear knock-on effect results in small changes for the 4 MeV alpha particle, a substantial effect is seen for both the 3 MeV and 14.5 MeV protons. The effect becomes more important as the electron temperature is increased. Accounting for both nuclear elastic scattering and subsequent slowing down of knock-on ions, a 14.5 MeV proton in a 75 keV ion temperature deuterium plasma will transfer 79% of its energy to 50 keV electrons compared to 93% when only coulomb scattering is assumed. At an electron temperature of 100 keV, the percentage of energy transferred to the electrons decreases to 51% compared to 85% with coulomb interactions only. The effect is clearly important in a plasma energy balance calculation. Overall, the net result is that lower $n\tau_E$ values are required to meet either the Lawson or ignition condition for the catalyzed d-d cycle.

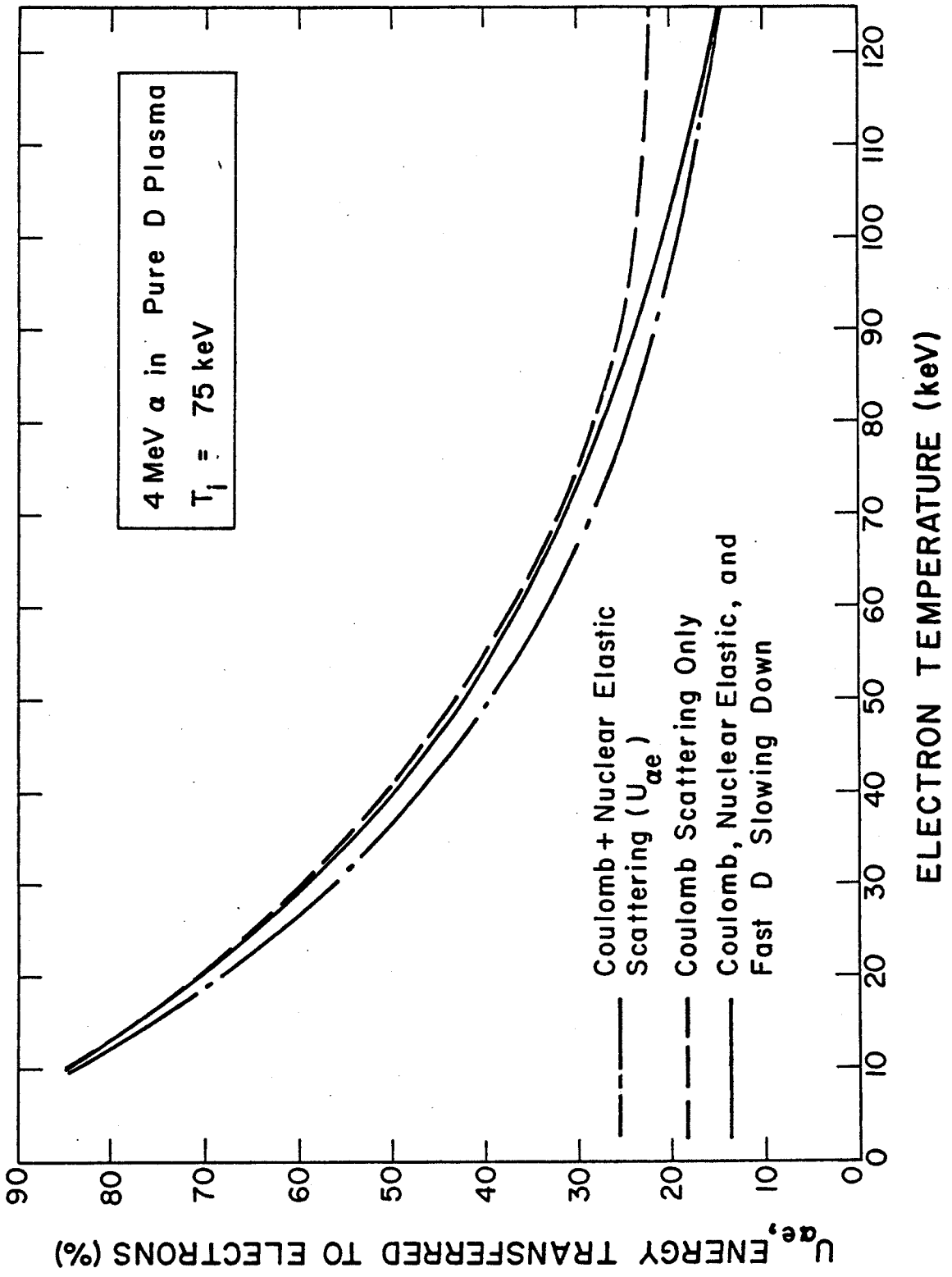
4 MeV α in Pure D Plasma
T_i = 75 keV
Coulomb + Nuclear Elastic Scattering ($U_{\alpha e}$)
Coulomb Scattering Only
Coulomb, Nuclear Elastic, and Fast D Slowing Down
$U_{\alpha e}$, ENERGY TRANSFERRED TO ELECTRONS (%)
ELECTRON TEMPERATURE (keV)
0
10
20
30
40
50
60
70
80
90
100
110
120

Fig. 5

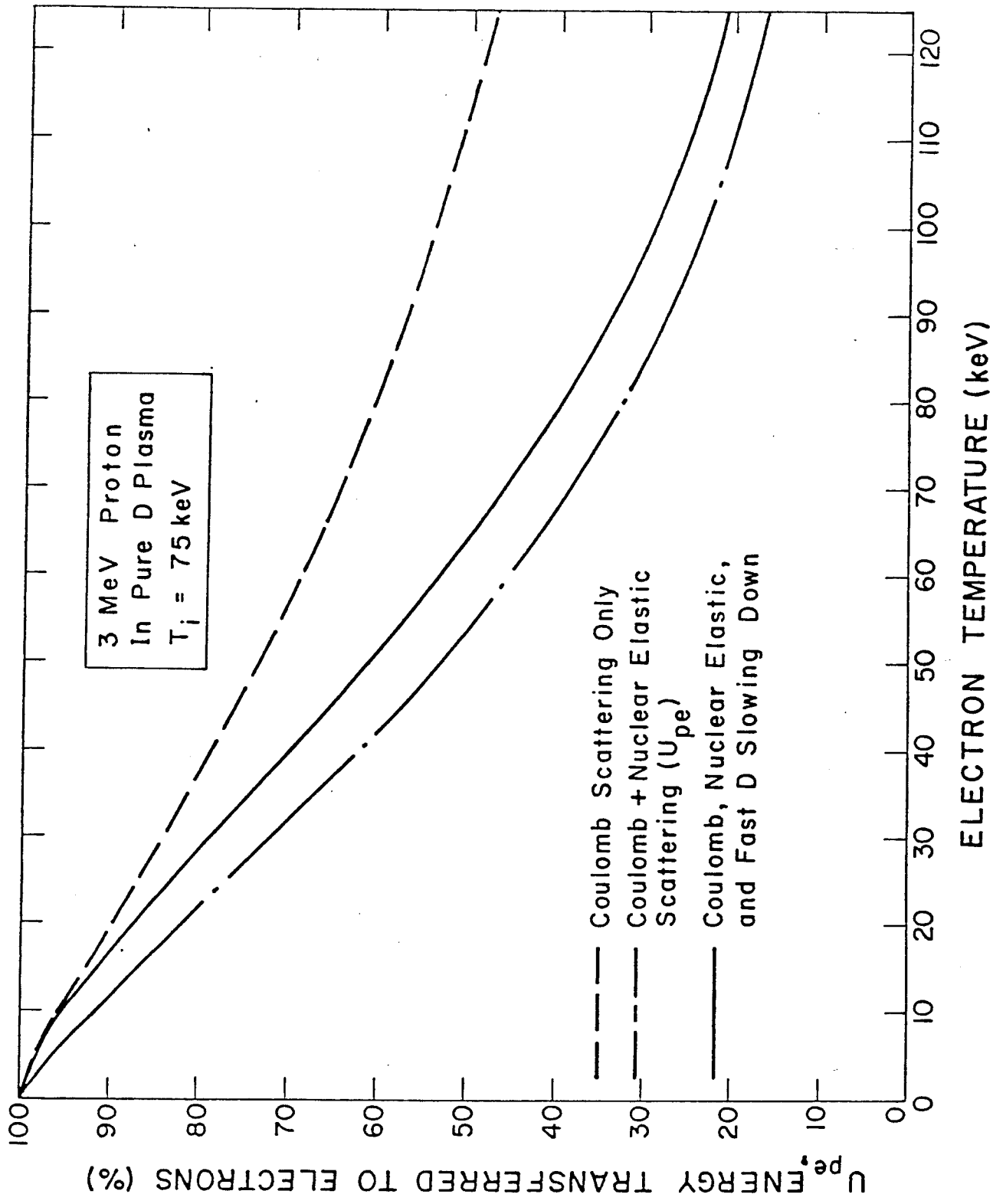
3 MeV Proton
In Pure D Plasma
T_i = 75 keV
Coulomb Scattering Only
Coulomb + Nuclear Elastic Scattering (U_{pe})
Coulomb, Nuclear Elastic, and Fast D Slowing Down
U_{pe}, ENERGY TRANSFERRED TO ELECTRONS (%)
ELECTRON TEMPERATURE (keV)
0
10
20
30
40
50
60
70
80
90
100
110
120

Fig. 6

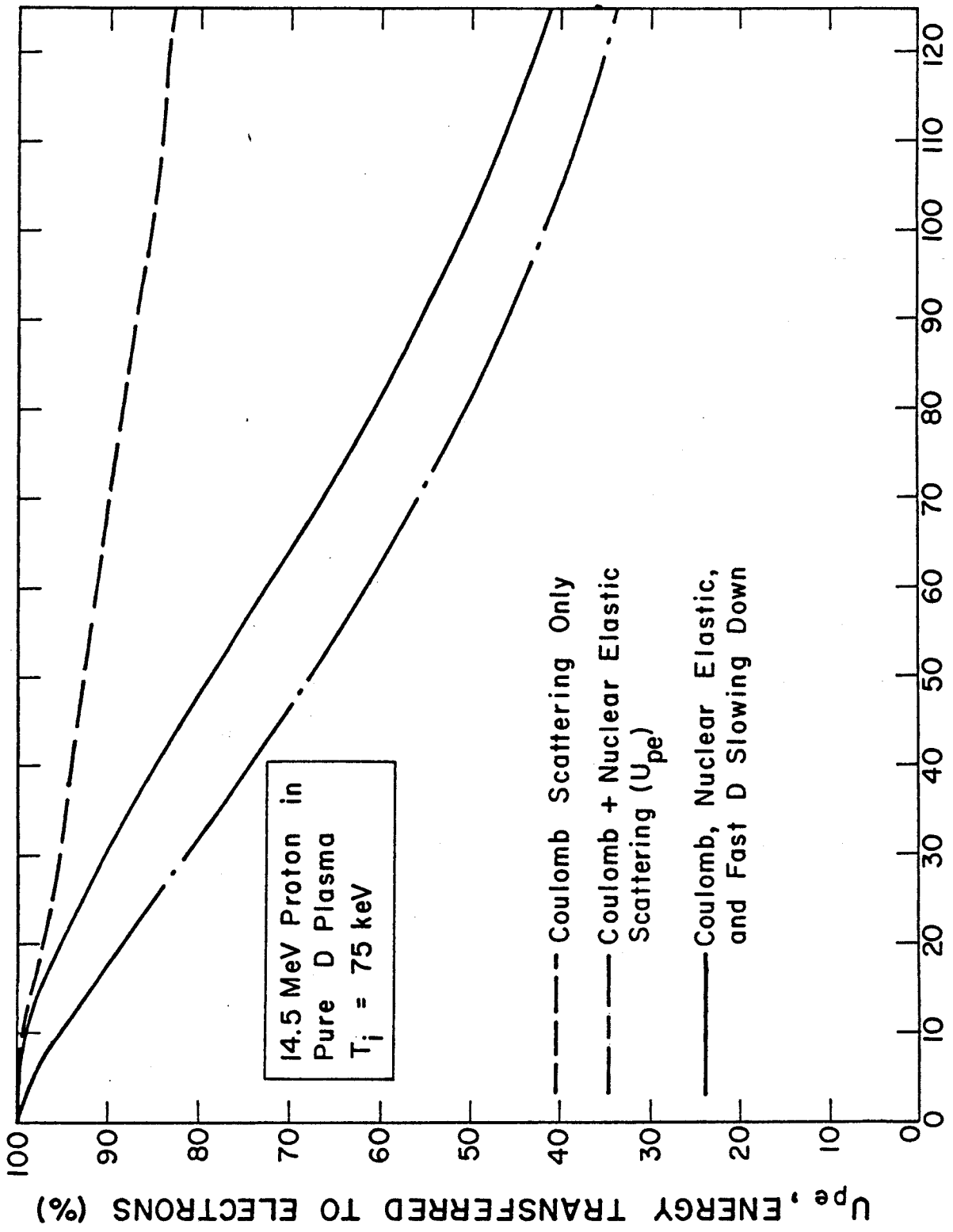
14.5 MeV Proton in
Pure D Plasma
T_i = 75 keV
Coulomb Scattering Only
Coulomb + Nuclear Elastic
Scattering (U_{pe})
Coulomb, Nuclear Elastic,
and Fast D Slowing Down
U_{pe}, ENERGY TRANSFERRED TO ELECTRONS (%)
ELECTRON TEMPERATURE (keV)
0
10
20
30
40
50
60
70
80
90
100
110
120

Fig. 7

II. Charged Particle Cross Section Requirements for Advanced Fusion Fuel Cycle Analysis

In order to properly determine the potential of each fusion fuel cycle, the basic nuclear data for nuclei with atomic mass numbers less than 12 must be known accurately.

1. Required Nuclear Data

The nuclear data required to analyze advanced fuels include fusion reaction cross sections, reaction rate parameters such as $\langle\sigma v\rangle$, reaction probabilities for fast fusion products to react with various elements in the background plasma, and nuclear elastic and inelastic cross sections to determine the energy transfer from the energetic fusion products to the background ions and electrons. The reaction rate, R, for two reacting species, a and b, is:

$$R = \int d\bar{v}_a \int d\bar{v}_b \; f_a(\bar{v}_a)\; f_b(\bar{v}_b)\; \sigma(u)\; u \qquad (11)$$

where R is the number of reactions per unit volume per unit time, f_a and f_b are the distribution functions, σ is the reaction cross section, and u is the relative velocity, $u = |\bar{v}_a - \bar{v}_b|$. It is convenient to write R as $n_a n_b \langle\sigma v\rangle$, where the density of species a and b (n_a and n_b) are found from

$$n_i = \int f_i\,(\bar{v}_i)\; d\bar{v}_i \qquad (i=a,b). \qquad (12)$$

The reaction rate parameter, $\langle\sigma v\rangle$, depends on the form of the normalized distribution functions $\hat{f}_i(\bar{v}_i) = \frac{1}{n_i} f_i(\bar{v}_i)$:

$$\langle\sigma v\rangle = \int d\bar{v}_a \int d\bar{v}_b \, \hat{f}_a(\bar{v}_a) \, \hat{f}_b(\bar{v}_b) \, \sigma(u) \, u \, . \tag{13}$$

If $\hat{f}_i(\bar{v}_i)$ is the Maxwellian distribution,

$$\hat{f}_i(\bar{v}_i) = \left(\frac{m_i}{2\pi KT}\right)^{3/2} \exp\left(-m_i v_i^2/2KT\right) , \tag{14}$$

the integral in Eqn. (13) can be expressed as:

$$\langle\sigma v\rangle = 4\pi \int_0^\infty u^2 \, du \left(\frac{\mu}{2\pi KT}\right)^{3/2} \exp\left(\frac{-\mu u^2}{2KT}\right) \sigma(u) u \, , \tag{15}$$

where μ is the reduced mass. Using $E = 1/2\mu u^2$, Eqn. (5) becomes

$$\langle\sigma v\rangle = \sqrt{\frac{8}{\pi\mu}} \left(\frac{1}{KT}\right)^{3/2} \int_0^\infty E \, \sigma(E) \exp\left(-E/KT\right) dE \, . \tag{16}$$

The ion temperature in an advanced fuel cycle fusion plasma may reach 500 keV. One clearly would like to know the reaction cross section, $\sigma(E)$, up to an energy at least 4 KT (or 2 MeV in the most extreme case) to analyze fusion reactions among species with a Maxwellian distribution. In addition, nuclear scattering events between energetic fusion products and the background Maxwellian can transfer significant energy (> 1 MeV) to the struck particle thereby promoting it to higher energy where it is typically more reactive. In short, cross sections are required not just to

an energy of 4-5 KT but to the energy of fusion reaction products. The p-^{6}Li cycle is particularly useful to demonstrate this requirement.

The primary reactions of this fuel cycle are:

$$p + {}^{6}Li \rightarrow {}^{3}He\ (2.3\ MeV) + \alpha\ (1.7\ MeV) \quad (17)$$

$${}^{3}He + {}^{6}Li \rightarrow p\ (11.3\ MeV) + 2\alpha\ (2.81\ MeV) \quad (18a)$$

$$\rightarrow p + {}^{8}Be\ (\text{various nuclear levels}) \quad (18b)$$

$$\rightarrow d\ (.088\ MeV) + {}^{7}Be\ (.026\ MeV) \quad (18c)$$

Secondary and tertiary reactions include:

$$\rightarrow n + {}^{7}Be\ (.42\ MeV) \quad (19a)$$

$$d + {}^{6}Li \begin{cases} \rightarrow p\ (4.4\ MeV) + {}^{7}Li\ (.63\ MeV) & (19b) \\ \rightarrow p\ (1.6\ MeV) + t + \alpha & (19c) \\ \rightarrow n + {}^{3}He + \alpha & (19d) \end{cases}$$

$$\rightarrow 2\alpha\ (11.2\ MeV) \quad (19e)$$

$$d + {}^{3}He \rightarrow p\ (14.6\ MeV) + \alpha\ (4.7\ MeV) \quad (20)$$

$$d + d \begin{cases} \rightarrow n + {}^{3}He\ (.82\ MeV) & (21a) \\ \rightarrow p\ (3\ MeV) + t\ (1.01\ MeV) & (21b) \end{cases}$$

$$d + {}^{7}Be \rightarrow p\ (11.2\ MeV) + 2\alpha\ (2.8\ MeV) \quad (22)$$

$$d + t \rightarrow n + {}^{4}He\ (3.5\ MeV) \quad (23)$$

$$t + {}^{3}He \begin{cases} \rightarrow d\ (9.6\ MeV) + \alpha\ (4.8\ MeV) & (24a) \\ \rightarrow p + n + \alpha & (24b) \end{cases}$$

$${}^{3}He + {}^{3}He \rightarrow 2p\ (5.7\ MeV) + \alpha\ (1.4\ MeV) \quad (25)$$

$${}^{3}He + {}^{7}Be \rightarrow 2p\ (4.5\ MeV) + 2\alpha\ (1.1\ MeV) \quad (26)$$

$$t + {}^{7}Be \rightarrow p\ (4.2\ MeV) + 2\alpha \quad (27)$$

$$d + {}^{7}Li \rightarrow n + 2d\ (2.52\ MeV) \quad (28)$$

In addition there are at least thirty side reactions and thirteen $^{6}Li + {}^{6}Li$ exothermic reactions which produce elements from H to ^{12}C and neutrons. Many of the fusion reaction products are energetic and may react with elements in the background plasma prior to completely slowing down (fast fusion or two-component fusion events). Including these fast fusion events is crucial, particularly for cycles that are propagating. Some important propagating fusion reaction sequences in the p-^{6}Li cycle (the fast particle has a bar over the element's designation) include:

$$\left\{\begin{array}{l} \bar{p} + {}^{6}Li \rightarrow {}^{3}\overline{He} + \alpha \\ {}^{3}\overline{He} + {}^{6}Li \rightarrow \bar{p} + 2\alpha \\ \bar{p} + {}^{6}Li \rightarrow {}^{3}\overline{He} + \alpha \\ \vdots \end{array}\right\} \quad (29) \qquad \left\{\begin{array}{l} \bar{p} + {}^{6}Li \rightarrow {}^{3}\overline{He} + \alpha \\ {}^{3}\overline{He} + d \rightarrow \bar{p} + \alpha \\ \bar{p} + {}^{6}Li \rightarrow {}^{3}\overline{He} + \alpha \\ \vdots \end{array}\right\} \quad (30)$$

$$\left\{\begin{array}{l} \bar{p} + {}^{6}Li \rightarrow {}^{3}\overline{He} + \alpha \\ {}^{3}\overline{He} + {}^{6}Li \rightarrow \bar{d} + {}^{7}Be \\ \bar{d} + {}^{6}Li \rightarrow \bar{p} + {}^{7}Li \\ \bar{p} + {}^{6}Li \rightarrow {}^{3}\overline{He} + \alpha \\ \vdots \end{array}\right\} \quad (31) \qquad \left\{\begin{array}{l} \bar{p} + {}^{6}Li \rightarrow {}^{3}\overline{He} + \alpha \\ {}^{3}\overline{He} + {}^{6}Li \rightarrow \bar{d} + {}^{7}Be \\ \bar{d} + {}^{7}Be \rightarrow \bar{p} + 2\alpha \\ \bar{p} + {}^{6}Li \rightarrow {}^{3}\overline{He} + \alpha \\ \vdots \end{array}\right\} \quad (32)$$

and there are others. See eq. 17-28 for the energies of the reaction products.

Nuclear elastic scattering of the energetic products with the background plasma produces additional energetic particles which can undergo fast fusion and further propagate the reaction. Therefore, the reaction cross section for the various channels and nuclear elastic scattering cross sections are required up to about 20 MeV.

2. Status of Nuclear Data for Advanced Fusion Fuel Cycle Analysis

The literature has been examined through October 1979. All data for a given reaction were examined for consistency. In general the uncertainties or inconsistencies ranged from 10% to as much as an order of magnitude. Cross sections for some of the reaction branches have either been partially measured or not measured at all. In the reactions ^{3}He-^{6}Li and d-^{7}Be, for example, recent measurements at ANL indicate that the total reaction cross section may be 10 to 50 times larger than previously reported values. For other reactions, such as ^{3}He with ^{7}Be, the data is nonexistent.

The status of nuclear data is summarized in matrix form in Tables 2, 3 and 4. The asterisk (*) indicates the reaction is important for fusion fuel cycle analysis; the check (√) indicates the data for that reaction are reasonably consistent; while the cross (X) indicates the existing data are eigher inconsistent or have large error bars. References are given in the parentheses. The numbers followed by MeV give the energy range over which data have been measured. A literature search for nuclear inelastic cross sections is in progress.

The data for several of the major fusion reactions will now be examined in greater detail.

(1) The d-d Reactions

$$d + d \rightarrow n + {}^{3}He \qquad Q = 3.269 \text{ MeV} \qquad (33)$$

$$d + d \rightarrow p + t \qquad Q = 4.033 \text{ MeV} \qquad (34)$$

Liskien and Paulsen[461] have summarized and evaluated the cross section measurements for E_d = .013 - 10 MeV. The data and evaluation are shown in Fig. 8. This is adequate for fusion fuel cycle analysis.

TABLE 2

	p	d	t	^{3}He	^{4}He
d	ELASTIC (1 - 20) σ (E, θ) 0.2 - 30. MeV * ✓ REACTION (———) ———	ELASTIC (46 - 49) σ (E, θ) 2. - 20. MeV * ✓ REACTION (50 -90) σ (E) or σ (E, θ) 0.013 - 14. MeV	S	S	ELASTIC (164 - 178) σ (E, θ) 0.3 - 20. MeV * ✓ REACTION (———) ———
t	ELASTIC (21 - 30) σ (E,θ) 0.05 - 8.3 MeV * ✓ REACTION (31 - 45) σ (E) orσ (E,θ) 1.0 - 10. MeV	ELASTIC (91 - 93) σ (E, θ) 0.013 - 10. MeV * ✓ REACTION (94 - 112) σ (E) or σ (E, θ) 0.01 - 15. MeV	ELASTIC (141 - 142) σ (E, θ) 1.58 - 2. MeV X REACTION (143 - 146) σ (E) or σ (E, θ) 0.04 - 2.2 MeV	S	ELASTIC (179 - 182) σ (E, θ) 1.2 - 18.2 MeV * X REACTION (———) ———
^{3}He	ELASTIC (126 - 140) σ (E, θ) 0.1 - 20. MeV * ✓ REACTION (———) ———	ELASTIC 113 - 116 σ (E, θ) 0.38 - 20. MeV * ✓ REACTION (117 - 125) σ (E) or σ (E, θ) 0.25 - 15. MeV	ELASTIC (147 -148) σ (E,θ) 5. - 19. MeV X REACTION 149 - 154 σ (E) or σ (E, θ) .15 - 1.9 MeV	ELASTIC (155 - 158) σ (E, θ) 5. - 20. MeV * ✓ REACTION (159 - 163) σ (E) or σ (E, θ) 0.06 - 2.2 MeV	ELASTIC (183 - 190) σ (E, θ) 1.72 - 20. MeV * X REACTION (———) ———

TABLE 3

	p	d	t	^{3}He	^{4}He
^{6}Li	ELASTIC (191 - 196) $\sigma(E, \theta)$ 0.5 - 16. MeV ✱ ✓ REACTION (197 - 210) $\sigma(E, \theta)$ 0.14 - 12. MeV	ELASTIC (211 - 213) $\sigma(E, \theta)$ 2. - 7. MeV ✱ ✓ REACTION (213 - 225) $\sigma(E, \theta)$ 0.1 - 1. MeV	ELASTIC (——) No measurement X REACTION (226 - 230) $\sigma(E, \theta)$ 0.3 - 20. MeV	ELASTIC (231) $\sigma(E, \theta)$ 8. - 20. MeV ✱ X REACTION 232 - 245 $\sigma(E, \theta)$ or $\sigma(E)$ 1.2 - 4.2 MeV	ELASTIC (246 - 250) $\sigma(E, \theta)$ 2. - 7.5 MeV REACTION (——) ——
^{7}Li	ELASTIC (251 - 254) $\sigma(E, \theta)$ 0.4 - 20. MeV X REACTION (255 - 285) $\sigma(E, \theta)$ or $\sigma(E)$ 0.8 - 15. MeV	ELASTIC (286) $\sigma(E, \theta)$ 0.4 - 1.8 MeV X REACTION (287 - 300) $\sigma(E)$ or $\sigma(E, \theta)$ 0.6 - 2.6 MeV	ELASTIC (——) No measurement X REACTION (301 - 310) $\sigma(E, \theta)$ 0.23 - 2.5 MeV	ELASTIC (311) $\sigma(\theta)$ 11. MeV X REACTION (312 - 325) $\sigma(E, \theta)$ 0.8 - 6. MeV	ELASTIC (326 - 330) $\sigma(E, \theta)$ 1.6 - 20. MeV REACTION (——) ——
^{7}Be	ELASTIC (——) No measurement X REACTION (——) ——	ELASTIC (——) No measurement ✱ X REACTION (331-332) $\sigma(E, \theta)$ 0.8 - 1.7 MeV	ELASTIC (——) No measurement X REACTION (306) No measurement $\langle \sigma V \rangle$ Estimated	ELASTIC (——) No measurement ✱ X REACTION (306) No measurement $\langle \sigma V \rangle$ Estimated	ELASTIC (——) No measurement REACTION (——) ——

TABLE 4

	p	d	t	^{3}He	^{4}He
^{9}Be	ELASTIC (333 - 340) σ (E, θ) 0.2 - 10. MeV ✓ REACTION (341 - 345) σ (E,θ) 0.028 - 2.0 MeV	ELASTIC (346 - 350) σ (E, 90^{o}) 0.4 - 7. MeV ✓ REACTION (351 -370) σ (E) or σ(E, θ) 0.15 - 19. MeV	ELASTIC (371, 372) σ(E, θ) 0.6 - 2.1 MeV ✓ REACTION (371, 372) σ(E, θ) 0.52 - 2.1 MeV	ELASTIC (373 - 375) σ(E, 45^{o}) or σ (E,90^{o}) 1.2 - 20. MeV X REACTION (376 - 380) σ (E, θ) 1.6 - 20. MeV	ELASTIC (381 - 384) σ (E, θ) 1.4 - 20. MeV REACTION (———) ———
^{10}B	ELASTIC (385 - 387) σ (E, θ) 0.15 - 10.5 MeV X REACTION (388 - 390) σ(E, θ) 0.06 - 6.3 MeV	ELASTIC (391 - 393) σ (E, θ) 1. - 16. MeV X REACTION (394 - 415) σ (E) or σ (E, θ) 0.14 - 12. MeV	ELASTIC (416 - 418) σ (E, θ) 1.5 - 3.3 MeV X REACTION (416) σ (E) 0.8 - 2.0 MeV	ELASTIC (419 - 423) σ(E, θ) 4. - 20. MeV X REACTION (424 - 430) Excitation function 2. - 19. MeV	ELASTIC (431 - 433) Excitation function 2. - 20. MeV REACTION (———) ———
^{11}B	ELASTIC (———) No data reported ✳ X REACTION (434 - 440) σ (E) or σ (E, θ) 0.17 - 10. MeV	ELASTIC (———) No data reported X REACTION (441 - 453) σ (E) or σ (E, θ) 0.3 - 10. MeV	ELASTIC (———) No data reported X REACTION 454, 455 σ (E, θ) 1.0 - 2.1 MeV	ELASTIC (———) No data reported X REACTION (456 - 460) Excitation function or σ (E) 0.9 - 18. MeV	ELASTIC (———) No data measurered below 27. MeV REACTION (———) ———

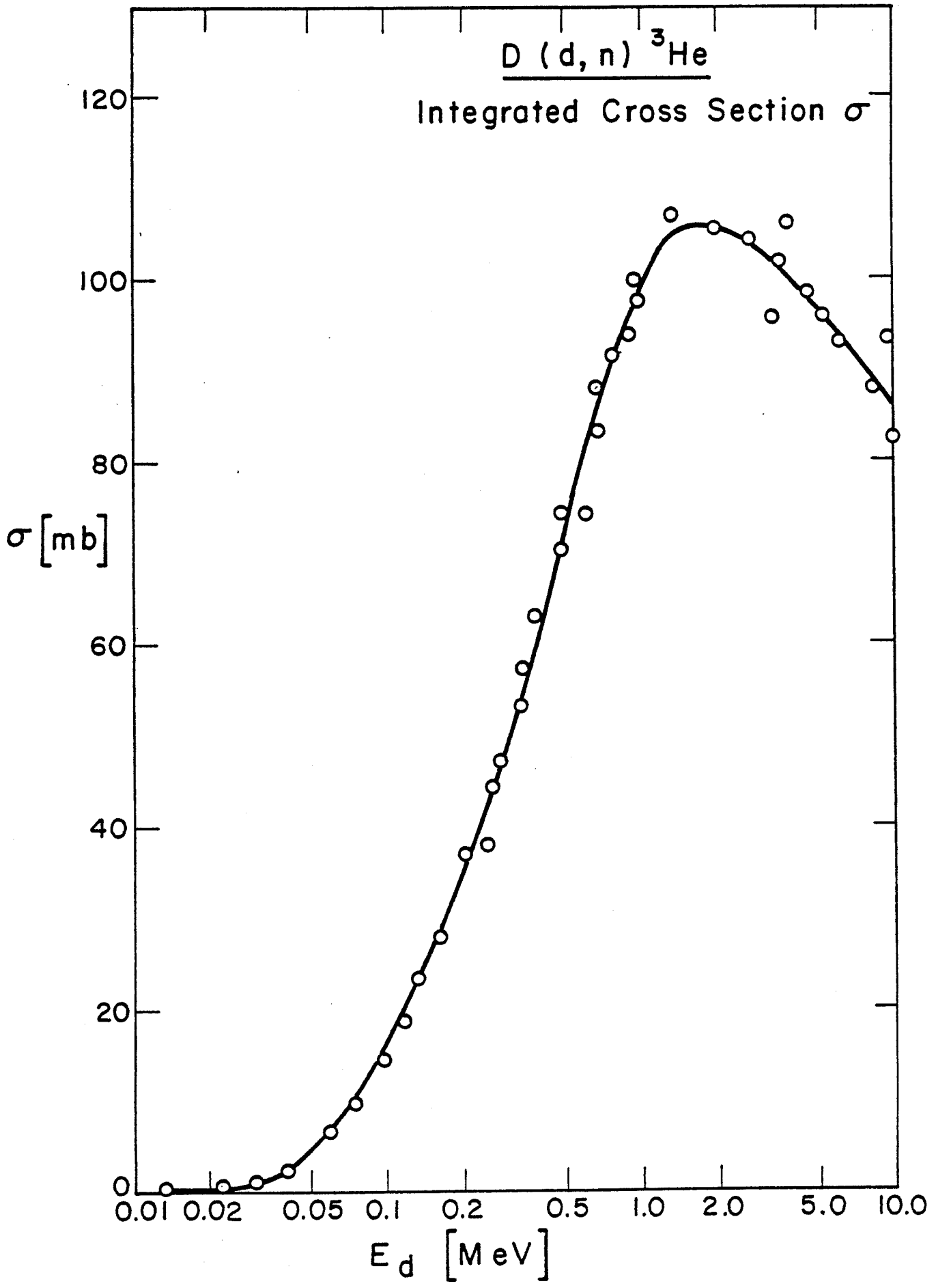
D (d, n) ³He
Integrated Cross Section σ
120
100
80
60
40
20
0
σ [mb]
0.01
0.02
0.05
0.1
0.2
0.5
1.0
2.0
5.0
10.0
E d [MeV]

Fig. 8

(2) The p-t Reaction

$$t + p \rightarrow n + {}^{3}He \qquad Q = -.764 \text{ MeV} \qquad (35)$$

Cross section measurements have been evaluated by Liskien and Paulsen.[462] The angular distribution measurements are inconsistent with one another. Most of the integrated cross section measurements are within 15% of the recommended values. Experimental values for E_p = 1.0 - 10 MeV are shown in Fig. 9. This data is adequate for fusion fuel cycle analysis.

(3) The d-t Reactions

$$t + d \rightarrow n + \alpha \qquad Q = 17.590 \text{ MeV} \qquad (36)$$

There has been only one measurement since 1960. The cross section measurements have been evaluated[463] and indications are that a number of reported angular distributions are not satisfactory at energies above 5 MeV. Most of the integrated cross section measurements are within 10% of the recommended values. In general, the data is adequate for fusion fuel cycle analysis.

(4) The d-^{3}He Reaction

$$^{3}He + d \rightarrow p + \alpha \qquad Q = 18.35 \text{ MeV} \qquad (37)$$

There have been no measurements since 1960. A pronounced resonance occurs at E_d = 430 keV with $\Gamma \sim 450$ keV. The experimental data disagree in the neighborhood of this resonance (~25%). However, analysis by Hale[464] suggests that the recommended values are very good. Thus, the cross sections are adequate for fusion fuel cycle analysis.

(5) The ^{3}He-^{3}He Reactions

$$^{3}He + {}^{3}He \rightarrow p + {}^{5}Li \qquad Q = 10.890 \text{ MeV} \qquad (38)$$

$$\hookrightarrow p + \alpha$$

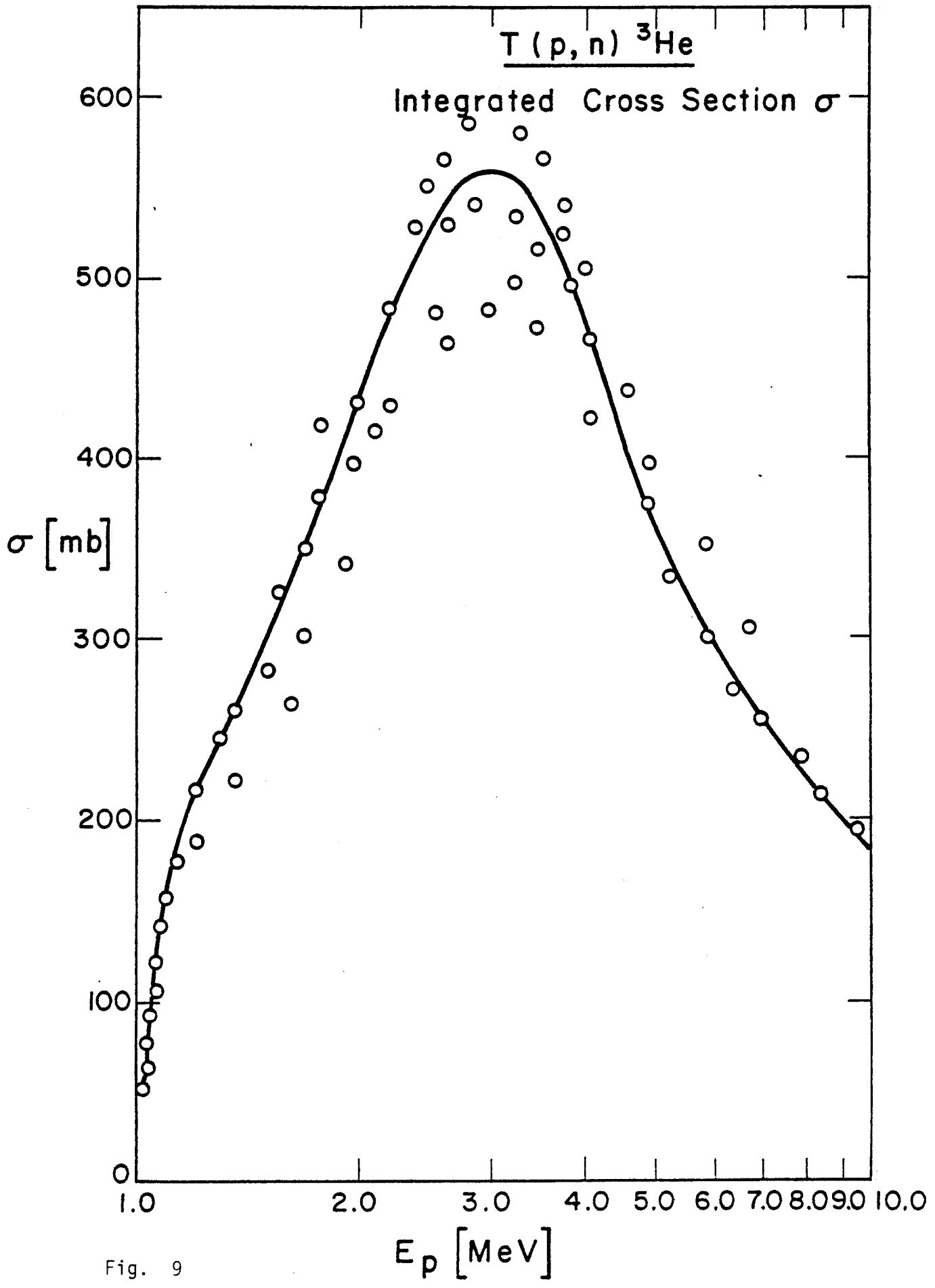
T (p, n) 3He
Integrated Cross Section σ
600
500
400
300
200
100
0
σ [mb]
1.0
2.0
3.0
4.0
5.0
6.0
7.0
8.0
9.0
10.0
Ep [MeV]

Fig. 9

$$^{3}He + {}^{3}He \rightarrow 2p + \alpha \qquad Q = 12.86 \text{ MeV} \qquad (39)$$

A study of the proton spectrum indicates that the reaction proceeds mainly via a direct mechanism and the ^{5}Li channel. However, the branching ratio is not firmly established, particularly at low energy.

(6) The p-^{6}Li Reaction

$$^{6}Li + p \rightarrow {}^{3}He + \alpha \qquad Q = 4.023 \text{ MeV} \qquad (40)$$

The cross section measurements for E_p = .14-3 MeV by Elwyn et al.[197] appear to be definitive. The earlier measurements are inconsistent with one another as shown in Fig. 10. Cross section measurements for E_p = 3 to 12 MeV have been made recently by Gould et al.[198] The measurements for E_p = 62 to 188 keV deviate from an S-wave Gamow plot above ~130 keV.

(7) The d-^{6}Li Reactions

$$d + {}^{6}Li \rightarrow n + {}^{7}Be \qquad Q = 3.380 \text{ MeV} \qquad (41)$$

$$\rightarrow p + {}^{7}Li \qquad Q = 4.026 \text{ MeV} \qquad (42)$$

$$\rightarrow p + t + \alpha \qquad Q = 2.561 \text{ MeV} \qquad (43)$$

$$\rightarrow n + {}^{3}He + \alpha \qquad Q = 1.796 \text{ MeV} \qquad (44)$$

$$\rightarrow 2\alpha \qquad Q = 22.374 \text{ MeV} \qquad (45)$$

The recent measurements for E_d = .1 - 1 MeV by Elwyn et al.[214] are definitive. Other measurements differ sharply with one another, even in recent experiments.[218] Cross section measurements for E_d > 1 MeV are needed for a complete analysis.

(8) The ^{3}He-^{6}Li Reactions

$$^{6}Li + {}^{3}He \rightarrow p + {}^{8}Be(g.s.) \qquad Q = 16.787 \text{ MeV} \qquad (46)$$

$$\downarrow 2\alpha$$

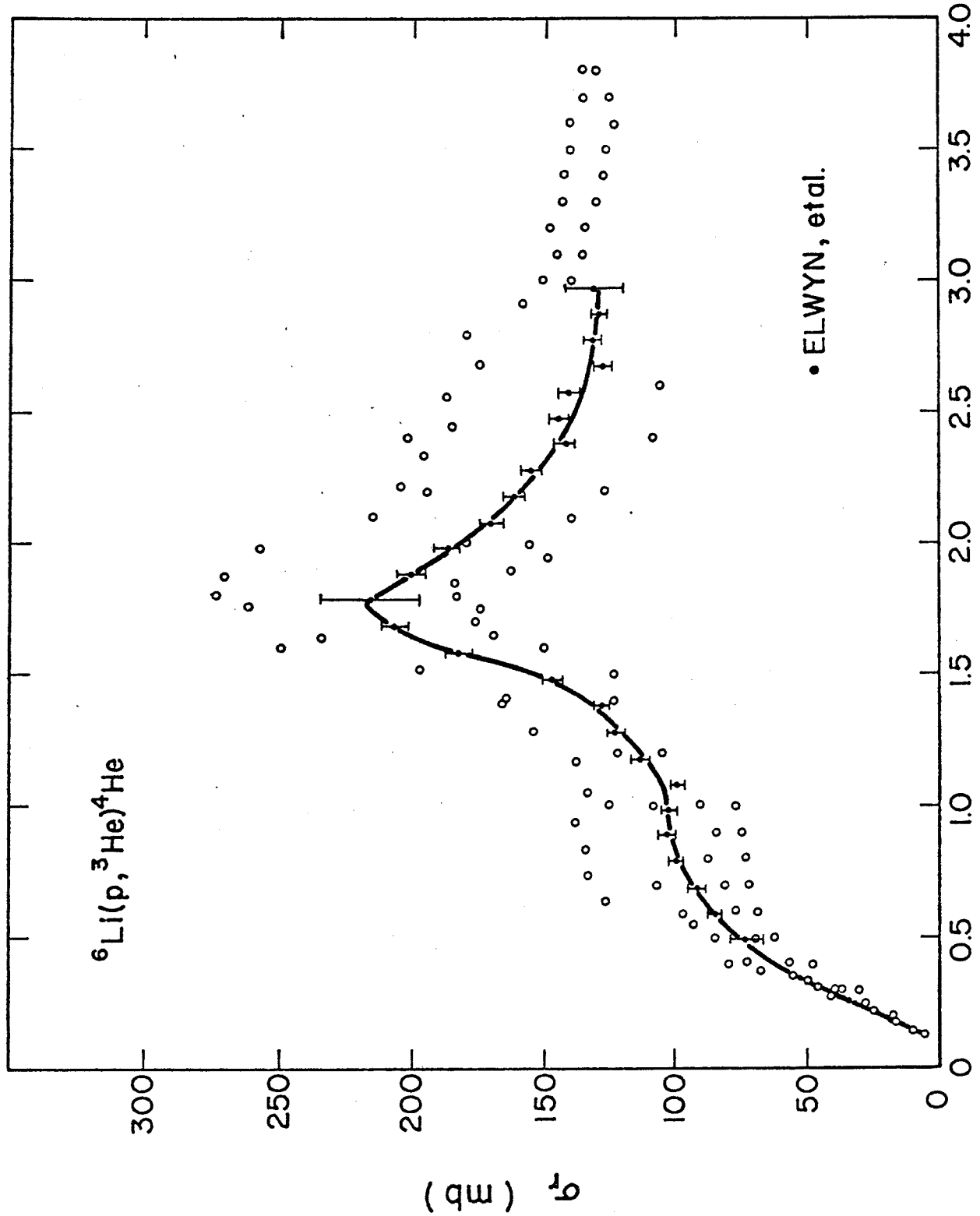
$^6Li(p,^3He)^4He$
• ELWYN, etal.
σ_r (mb)
E_p (MeV)
0
50
100
150
200
250
300
0.5
1.0
1.5
2.0
2.5
3.0
3.5
4.0

Fig. 10

$\rightarrow p + {}^{8}Be(2.94)$ $\quad Q = 13.847$ MeV (47)

$\quad\quad \hookrightarrow 2\alpha$

$\rightarrow p + {}^{8}Be(11.4)$ $\quad Q = 5.387$ MeV (48)

$\quad\quad \hookrightarrow 2\alpha$

$\rightarrow p + {}^{8}Be(16.63)$ $\quad Q = .157$ MeV (49)

$\quad\quad \hookrightarrow 2\alpha$

$\rightarrow p + {}^{8}Be(16.92)$ $\quad Q = -.1325$ MeV (50)

$\quad\quad \hookrightarrow 2\alpha$

$\rightarrow p + {}^{8}Be(17.64)$ $\quad Q = -.853$ MeV (51)

$\rightarrow p + 2\alpha$ $\quad Q = 16.88$ MeV (52)

$\rightarrow \alpha + {}^{5}Li$ $\quad Q = 14.91$ MeV (53)

$\quad\quad \hookrightarrow p + \alpha$

$\rightarrow d + {}^{7}Be$ $\quad Q = .1126$ MeV (54)

$\rightarrow d + {}^{7}Be(.43)$ $\quad Q = -.31$ MeV (55)

$\rightarrow 2p + {}^{7}Li$ $\quad Q = -.468$ MeV (56)

A measurement is in progress by A. Elwyn et al., at the Argonne National Laboratory.[465] The earlier measurements are not complete. At least 5 nuclear levels in ^{8}Be can be excited. It is expected that the reaction cross section to all branches will be at least a factor of 10 larger than those now known. For example, at $E_{^{3}He} = 3.5$ MeV, Gould et al.[245] measured $\sigma_r \approx$ 10-12 mb for the ^{8}Be(g.s.) branch, $\sigma_r \approx 55$ mb for the ^{8}Be(2.94 MeV) branch and estimated $\sigma_r \approx 42$ mb for the continuum breakup reaction, Elwyn et al., indicate values could be $\sigma_r \approx$ 30-50 mb for the ^{8}Be(16.63 MeV) branch, $\sigma_r \approx$ 20-40 mb for the ^{8}Be(16.9 MeV) branch and $\sigma_r \approx 400$ mb for the d + ^{7}Be branch.

(9) The d-^{7}Be Reactions

There have been no measurements since 1960, since ^{7}Be is somewhat rare. d + ^{7}Be reacts via the same compound nucleus as ^{3}He + ^{6}Li. Therefore, it will have the same reaction channels as ^{3}He + ^{6}Li except for eqns. (54) and (55). Since the existing data are only for the eqn. (46) and (47) branches, measurements for each branch stated above are required. However, in lieu of an experimental determination of σ, a standard 9-nucleon R-matrix calculation can give good estimated values, provided that the cross sections of each branch of ^{3}He + ^{6}Li reaction are given.

(10) The p-^{11}B Reaction

$$^{11}B + p \rightarrow \alpha + {}^{8}Be \qquad Q = 8.590 \text{ MeV} \qquad (57)$$

$$^{11}B + p \rightarrow 3\alpha \qquad Q = 8.682 \text{ MeV} \qquad (58)$$

The most recent cross section measurements for E_p = 0.08 - 1.4 MeV by Davidson et al.[434] appear to be definitive. There are 7 pronounced resonances in the range, E_p = .1 - 5 MeV. The energy of the resonances, the cross sections at each resonance peak, and the width of each resonance are summarized in Table 5. The cross sections are uncertain above 2 MeV and should be measured again.

Table 5

Parameters for p-^{11}B Resonances

Resonance Energy E_p (MeV)	Cross Section at Resonance Peak (mb)	Resonance Width Γ (keV)
.172	28	10
.64	800	300
1.39	180	1160
1.98	133 - 132	100
2.62	200 - 347	320
3.75	200 - 348	1100
4.93	130 - 210	180

CHAPTER II

REFERENCES

1. Taschek, Phys. Rev. 61 (42) 13.
2. Sherr et al., Phys. Rev 72 (47) 662.
3. Kocher and Clegg, Nucl. Phys. A132 (69) 455.
4. Wilson et al., Nucl. Phys. A130 (69) 624.
5. Kikuchi et al., J. Phys. Soc. Japan 15 (60) 9.
6. Kerman, Phys. Rev. 107 (57) 200.
7. Kiceleva et al., Ukr. Fiz. Zh. 4 (71) 83.
8. Cahill et al., Phys. Rev. C4 (71) 83.
9. Cadwell and Richardson, Phys. Rev. 98 (55) 28.
10. Allred and Rosen, Phys. Rev. 79 (50) 227.
11. Karr et al., Phys. Rev. 81 (51) 37, 78 (50) 292.
12. Allred et al., Phys. Rev. 88 (52) 433.
13. Simpson, Thesis, Rice Univ., Houston (65).
14. Grötzschel et al., Nucl. Phys. A176 (71) 261.
15. Brolley Jr. et al., Phys. Rev. 117 (60) 1307.
16. Mather, Phys. Rev. 88 (52) 1408.
17. Heither et al., Proc. Roy. Soc. A190 (47) 180.
18. Brown et al., Phys. Rev. 88 (52) 253.
19. Tuve et al., Phys. Rev. 50 (36) 806.
20. Bunker et al., Nucl. Phys. A113 (68) 461.
21. Balashko et al., Zh. Eksp. Teor. Fiz. 36 (59) 1937, JETP (Soviet Physics) 9 (59) 1378.
22. Baumann, J. Phys. Rad. 18 (57) 337.
23. Jarmie et al., Phys. Rev. 130 (63) 1987.
24. Balashko et al., JETP 19 (64) 1281.
25. Kurepin, Trudy of the Lebedev Phys. Inst., Vol. 33 (65) p.1 (Transl. by Consultant Bureau, N.Y. 66).
26. Jarmie and Allen, Phys. Rev. 114 (59) 176.
27. Hemmendinger et al., Phys. Rev. 79 (49) 1137.
28. Ennis and Hemmendinger, Phys. Rev. 95 (54) 772.
29. Brolley et al., Phys. Rev. 117 (60) 1307.
30. Classen et al., Phys. Rev. 82 (51) 589.
31. Seagrave, Proc. Conf. on Nuclear Forces and the Few Nuclear Problem , London (59) Vol. II, p.583.
32. Macklin and Gibbons, EANDC-50-S, Vol. I (65).
33. Willard et al., Phys. Rev. 90 (53) 865.
34. Jarmie and Seagrave LA-2014 (56).
35. Gibbons and Macklin, Phys. Rev. 114 (59) 571.
36. Batchelor et al., Rev. Sci. Instr. 26 (55) 1037.
37. Costello et al., Nucl. Sci. Eng. 39 (70) 409.
38. Vlasov et al., JETP 1 (55) 500.
39. Coon, Phys. Rev. 80 (50) 488.
40. Sayres et al., Phys. Rev. 122 (61) 1853.
41. Seagrave et al., Phys. Rev. 119 (60) 1981.
42. Bogdandov et al., JETP 9 (59) 440.
43. Stewart et al., Bull. Am. Phys. Soc. 1 (56) 93.
44. Wilson et al., Nucl. Phys. 27 (61) 421.
45. Goldberg et al., Phys. Rev. 122 (61) 1510.

46. Theus et al., Nucl. Phys. 80 (66) 273.
47. Bacher and Tombrello, Nucl. Phys. A113 (68) 557.
48. Wilson et al., Nucl. Phys. A126 (69) 193.
49. Cahill et al., CEN-Saclay Annual Report CEA-N 844 (67) 121.
50. Goldberg, Progress in Fast Neutron Physics (U. of Chicago Press 63).
51. Arnold et al., Phys. Rev. 93 (54) 483.
52. Booth et al., Proc. Phys. Soc. (London) A69 (56) 265.
53. NcNeill and Keyser, Phys. Rev. 81 (51) 602.
54. Ganeev et al., Atomnaya Energiya Suppl. 5 (57)21.
55. Preston, et al., Proc. Roy. Soc. (London) A226 (54) 206.
56. Chagnon and Owen, Phys. Rev. 101 (56) 798.
57. Hunter and Richards, Phys. Rev. 76 (49) 1445.
58. Ref. 40.
59. Brolley et al., Phys. Rev. 107 (57) 820.
60. Blair et al., Phys. Rev. 74 (48) 1599.
61. - 70. Not Used
71. Schulte et al., Nucl. Phys. A192 (72) 609.
72. Goldberg et al., Phys. Rev. 119 (60) 1992.
73. Thornton, Nucl. Phys. A139 (69) 25.
74. Brolley et al., Phys. Rev. 107 (57) 820.
75. Eliot et al., Proc. Roy. Soc. (London) 216 (53) 57.
76. Ref. 46
77. Kane, Nucl. Phys. 10 (59) 429.
78. Fuller et al., Phys. Rev. 108 (57) 91.
79. Volkov et al., Stomnaya Energiya Suppl. 5 (57)13.
80. Milone and Ricamo, Nuovo Cim. 22 (61) 116.
81. Cranberg et al., Phys. Rev. 104 (56) 1639.
82. Kerr and Anderson, Bull. Am. Phys. Soc. 13 (68) 564.
83. Daehnick and Fowler, Phys. Rev. 111 (58) 1309.
84. Ref. 43
85. Wilson et al., Bull. Am. Phys. Soc. 5 (60) 410.
86. Brill et al., Atomnaya Energiya 16 (64) 141.
87. Bame et al., Rev. Sci. Instr. 28 (57) 997.
88. Fowler and Brolley, Rev . Mod. Phys. 28 (56) 103.
89. Ref. 34
90. Defacio, Proc. 3rd Int. Symp. on Polarization Phenomena in Nuclear Reactions (71) 534 (U. of Wisconsin Press).
91. Stratton et al., Phys. Rev. 88 (52) 257.
92. Brolley et al., Phys. Rev. 120 (60) 905.
93. Allred et al., Phys. Rev. 88 (52) 425.
94. Conner et al., Phys. Rev. 88 (52) 468.
95. Ref. 51

96. Davidenks et al., J. Nucl. Energy 2 (57) 258 .
97 Balabanov et al., Atomnaya Energiya Suppl. 5 (57) 43.
98. Argo et al., Phys. Rev. 87 (52) 612.
99. Kobzev et al., Sov. J. Nucl. Phys. 3 (66) 774.
100. Bame and Perry, Phys. Rev. 107 (57) 1616.
101. Allen and Jarmie, Phys. Rev. 111 (58) 1129.
102. Hemmendinger and Argo, Phys. Rev. 98 (55) 70.
103. Galonsky and Johnson, Phys. Rev. 104 (56) 421.
104. Stewart et al., Phys. Rev. 119 (60) 1649.
105. Brill et al., Atomnaya Energiya 16 (64) 141.
106. Stratton and Freir, Phys. Rev. 88 (52) 261.
107. Goldberg et al., Phys. Rev. 122 (61) 164.
108. Simmons and Malanify, Bull. Am. Phys. Soc. 13 (68) 564.
109. Bretscher and French, Phys. Rev. 75 (49) 1154.
110. Allan and Poole, Proc. Roy. Soc. (London) A204 (50) 500.
111. Brolley et al., Phys. Rev. 82 (51) 502.
112. Paulsen and Liskien, Nucl. Phys. 56 (64) 394.
113. Brown et al., Phys. Rev. 96 (54) 80.
114. Tombrello et al., Phys. Rev. 154 (67) 935.
115. King and Smythe, Nucl. Phys. A183 (72) 657.
116. Baker et al., Nucl. Phys. A184 (72) 97.
117. Jarmie et al., LA-2014 (57).
118. Carlton, Thesis, U. of Georgia (70) Phys. Abst. 67885 (71).
119. Gruebler et al., Nucl Phys. A176 (71) 631.
120. Stewart et al., Phys. Rev. 119 (60) 1649.
121. Kunz, Phys. Rev. 97 (55) 456.
122. Bonner et al., Phys. Rev. 88 (52) 473.
123. Frier and Halmgren, Phys. Rev. 93 (54) 825.
124. Yarnel et al., Phys. Rev. 90 (53) 292.
125. Jarmie and Jett, Phys. Rev. C10(74) 145.
126. Hutson et al., Phys. Rev. C4 (71) 17.
127. Vanetsian and Fedchenko, Soviet J. of Atomic Energy 2 (57) 141.
128. Lovberg, Phys. Rev. 103 (56) 1393.
129. Igo and Leland, Phys. Rev. 154 (67) 950.
130. Brolley and Fowler, Fast Neutron Physics (60).
131. Rosen, Nuclear Forces and the Few Nuclear Problem (Pergamon 60) p. 481.
132. Brolley et al., Phys. Rev. 117 (60) 1307.
133. Sweetman, Phil. Mag. 46 (55) 358.
134. Artemov et al., JETP 10 (60) 474.
135. Clegg et al., Nucl. Phys. 50 (64) 621.
136. McDonald et al., Phys. Rev. 133 (64) B1178.
137. Tombrello et al., Nucl. Phys. 39 (62) 541.
138. Drigo et al., Nuovo Cim. 42B (66) 363.
139. Famularo et al., Phys. Rev. 93 (54) 928.
140. Kavanagh and Parker, Phys. Rev. 143 (66) 779.
141. Holm and Argo, Phys. Rev. 101 (56) 1772.
142. Frank and Grammel, Phys. Rev. 100 (55) 973A.
143. Agnew et al., Phys. Rev. 84 (51) 862.
144. Jarmie et al., Los Alamos Report 2014 (57).
145. Jarmie and Allen, Phys. Rev. 111 (58) 1121.

146. Strelenikov et al., Izv. Akad. Nauk USSR (Ser. Fiz.) 35 (71) 165.
147. Ivanovich et al., Nucl. Phys. A110 (68) 441.
148. Bacher et al., Nucl. Phys. A119 (68) 360.
149. Kuhn and Schlenk, Nucl. Phys. 48 (63) 353.
150. Moak, Phys. Rev. 92 (53) 383.
151. Youn et al., JETP 12 (61) 163.
152. Smith et al., Phys. Rev. 129 (63) 785.
153. Leland et al., Bull. Am. Phys. Soc. 10 (65) 51.
154. Kuhn and Schlenk, Joint Inst. Nucl Res. USSR Report No. P1197 (63).
155. Ref. 147 & Ref. 148
156. Tombrello and Bacher, Phys. Rev. 130 (63) 1108.
157. Jenkin et al., Phys. Rev. C1 (70) 1622.
158. Bacher et al., Bull. Am. Phys. Soc. 13 (68) 1366.
159. Dwarakanath, Phys. Rev. C9 (74) 805.
160. Dwarakanath and Winkler, Phys. Rev. C4 (71)1532.
161. Dwarakanath, Thesis, Caltech (69) Phys. Abstr. 39101 (70).
162. Slobodrian et al., Nucl. Phys. A194 (72) 577.
163. Good et al., Phys. Rev. 94 (54) 87.
164. Lauritsen et al., Phys. Rev. 92 (53) 1501.
165. Guggenheimer et al., Proc. Roy. Soc. A190 (47) 196.
166. Burge et al., Proc. Roy Soc. A210 (51) 534.
167. Galonsky et al., Phys. Rev. 98 (55) 586.
168. Alfred et al., Phys. Rev. 82 (51) 786.
169. Freemantle et al., Phil. Mag. 45 (54) 1090.
170. Artemov and Vlasov, JETP 12 (61) 1124.
171. Stewart et al., Phys. Rev. 128 (62) 707.
172. Rothe et al., Bull. Am. Phys. Soc. 8 (63) 537.
173. Ohlsen and Young, Nucl. Phys. 52 (64) 134.
174. Senhouse and Tombrello, Nucl. Phys. 57 (64)624.
175. Matons and Browne, Phys. Rev. 136 (64) B399.
176. Fukunaga et al., J. Phys. Soc. Japan 22 (67) 28.
177. Mani and Tarratts, Nucl. Phys. A107 (68) 624.
178.* Jett et al., Phys. Rev. C3 (71) 1769.
180. Allen and Jarmie, Phys. Rev. 111 (58) 1129.
181. Brolley et al., Nuclear Forces and the Few Nuclear Problem Vol. II, p. 455.
182. Tombrello and Phillips, Phys. Rev. 122(61)224.
183. Miller and Phillips, Phys. Rev. 112 (58) 2048.
184. Barnard et al., Nucl. Phys. 50 (64) 629.
185. Tombrello and Parker, Phys. Rev. 130 (63) 1112.
186. Spiger and Tombrello, Bull. Am. Phys. Soc. 9 (64) 703.
187. Chuang, Nucl. Phys. A174 (71) 399.
188. Spiger and Tombrello, Phys. Rev. 163 (67) 964.
189. Dunnil et al., Nucl. Phys. A93 (67) 201.
190. Ivanovich et al., Nucl. Phys. A110 (68) 441.
191. Harrison, Nucl. Phys. A92 (67) 253 and 260.
192. Harrison and Whitehead, Phys. Rev. 132 (63)2607.
193. Fasoli et al., Nuovo Cim. 34 (64) 1832.
194. Merchez et al., J. Physique 29 (68) 969.
195. Bashkin and Richards, Phys. Rev. 84 (51) 1124.

196. McCray, Phys. Rev. 130 (63) 2034.
197. Elwyn, Holland, Davids et al., accepted by Phys. Rev. C, to be published.
198. Gould et al., Nucl. Cross Section and Tech. NPP 425, 697.
199. Spinka et al., Nucl. Phys. A164 (71) 1.
200. Bowersox, Phys. Rev. 55 (39) 323.
201. Marion et al., Phys. Rev. 104 (56) 1402.
202. Field and Kunze, Nucl. Phys. A96(67) 513.
203. Beavmevielle, CEA-R-2624 (64).
204. Hub et al., Z. Phys. 252 (72) 332.
205. Varnagy et al., Nucl. Int. Methods 119 (74) 451.
206. Hooton and Ivanovich, AERE-R-7761 (74).
207. Johnston and Sargood, Nucl. Phys. A224 (74) 349.
208. Jeronymo et al., Nucl. Phys. 43 (63) 424.
209. Kibler, Phys. Rev. 152 (56) 932.
210. Gemeinhardt et al., Zeit, für Physik 197 (66) 58.
211. Paul and Lieb, Nucl. Phys. 53 (64) 465.
212. Bruno et al., J. Physique C1 (66) 85.
213. Black et al., Phys. Lett. 30B (69) 100.
214. Elwyn et al., Phys. Rev. C16 (77) 1744.
215. Risler et al., Nucl. Phys. A286 (77) 115.
216. Schier, et al., Nucl. Phys. 88 (66) 373.
217. McClenahan and Segal, Phys. Rev. C11 (75) 370.
218. Ruby et al., Nucl. Sci. Eng. 71 (79) 280.
219. Baggett et al., Phys. Rev. 85 (52).
220. Slattery et al., Phys. Rev. 108 (57) 809.
221. Bertrand et al., Saclay Report CEA-R-3428.
222. Whaling et al., Phys. Rev. 75 (49) 688.
223. Sawyer and Phillips, LA-1578.
224. Hirst et al., Phil. Mag. 45 (54) 762.
225. Elwyn et al., Phys. Rev. C19 (79) 592.
226. Pepper et al., Phys. Rev. 85 (52) 155.
227. Serov, et al., Soviet J. At. En. 12 (62) 1.
228. Valter, et al., Soviet J. At. En. 10 (61) 574.
229. Abramovich et al., Izv. Akad. Nauk SSSR (Ser. Fiz) 37 (73) 1967.
230. Ciric et al., Fizika (Yugoslavia) 4 (72) 40 and 193.
231. Ludecke et al., Nucl. Phys. A109 (68) 676.
232. Holmgren, Nuclear Research with Low Energy Accelerators, p. 213.
233. Mazari et al., Proc. 2nd Int. Conf. on Nuclidic Masses (63).
234. Reimann et al., Phys. Rev. Lett. 18 (67) 246.
235. Baker et al., Nucl. Phys. A184 (72) 97.
236. Reinmann et al., Can. J. Phys. 46 (68) 2241.
237. Treado et al., Bull. Am. Phys. Soc. 16 (71)1186.
238. Gagne et al., Bull. Am. Phys. Soc. 15 (70) 1695.
239. Vignon et al., J. Physique 30 (69) 913.
240. Tompson and Tripard, Phys. Rev. C5 (72) 1174.

241. Livesey and Piluso, Can. J. Phys. 52 (74) 1167.
242. Guichard et al., Nature 272, No. 5649 (78) 155.
243. Ref. 231 and Ref. 217
244. McClenahan, Thesis, Northwestern U. (74).
245. Gould and Boyce, Nucl. Sci. and Eng. 60 (76) 477.
246. Dearnaley et al., Nucl. Phys. 36 (62) 71.
247. Barnes et al., Bull. Am. Phys. Soc. 7 (62) 111.
248. Singh and Gemmell, Bull. Am. Phys. Soc. 10 (65) 538.
249. Meyer et al., Nucl. Phys. A101 (67) 114.
250. Balakrishnan et al., Nuovo Cim 1A (71) 205.
251. Warren et al., Phys. Rev. 91 (53) 917.
252. Malmberg, Phys. Rev. 101 (56) 114.
253. Kinsey and Stone, Phys. Rev. 103 (56) 972.
254. Gogny and Jean, Compt. Rend. 260 (65) 510.
255. Heydrenburg et al., Phys. Rev. 74 (48) 405.
256. Conrad et al., Nature 45 (58) 204.
257. Cavallaro et al., Nucl. Phys. 36 (62) 597.
258. Maxson, Phys. Rev. 128 (62) 1321.
259. Miller et al., Nucl. Phys. 54 (64) 155.
260. Madsen and Vedelsby, Nucl. Phys. 55 (64) 477.
261. Johnson et al., Phys. Rev. 77 (51) 413.
262. Taschek and Hemmendinger, Phys. Rev. 74 (48) 373.
263. Willard and Perston, Phys. Rev. 81 (51) 480.
264. Cranberg, LA-1654 (54).
265. Batchelor, Proc. Phys. Soc. A68(55)452.
266. Batchelor and Morrison, Proc. Phys. Soc. A68 (55) 1081.
267. Marion et al., Phys. Rev. 100 (55) 91.
268. Macklin and Gibbons, Phys. Rev. 109 (58) 105.
269. Newson et al., Phys. Rev. 108 (57) 1294.
270. Jarmie and Seagrave, LA-2014 (56).
271. Bogdanov et al., Soviet J. At. En. 3 (59) 907.
272. Gibbons and Macklin, Phys. Rev. 114 (59) 571.
273. Hisatake et al., J. Phys. Soc. Japan 15 (60)741.
274. Bevington et al., Phys. Rev. 121 (61) 871.
275. Nilsson, Ark. Fys. 19 (61) 289.
276. Borchers and Poppe, Phys. Rev. 129 (63) 2679.
277. Bair et al., Nucl. Phys. 53 (64) 209.
278. Buccino et al., Nucl. Phys. 53 (64) 375.
279. Austin, Bull. Am. Phys. Soc. 7 (62) 269.
280. Bergstroem et al., Ark. Fys. 34 (67) 153.
281. Lefevre and Din, Austr. J. Phys. 22 (69) 669.
282. Peetermans, Thesis, U. of Liege.
283. Elbakr et al., Nucl. Inst. Meth. 105 (72) 519.
284. Meadows and Smith, ANL-7938 (72).
285. Presser and Bass, Nucl. Phys. A182 (72) 321.
286. Ford, Phys. Rev. 136 (64) B953.
287. Sellschop, Phys. Rev. 119 (60) 251.
288. Chase et al., Phys. Rev. 127 (62) 859.
289. Schilling et al., Nucl. Phys. A263 (76) 389.
290. Kavanagh, Nucl. Phys. 15 (60) 411.
291. Bagget et al., Phys. Rev. 85 (52) 434.
292. McClenahan et al., Phys. Rev. C11 (75) 370.
293. Parker, Phys. Rev. 150 (66) 851.
294. Bashkin, Phys. Rev. 95 (54) 1012.

295. Valkovic et al., Nucl. Phys. A96(67) 241.
296. Garnir et al., Bull. Soc. R. Sci., Liege (Belgium) 42 (73) 195.
297. Crews, Phys. Rev. 82 (51) 100.
298. Serov et al., Soviet J. At. En. 12 (62) 1.
299. Valter et al., Soviet J. At. En. 10 (61) 574.
300. Arnold, In Proceedings, Cluster, Winnipeg (78) B8.
301. Valter et al., Soviet J. At. En. 10 (61) 577.
302. Seltz and Magnac-Valette, Compt. Rend. 251 (60) 2006.
303. Serov and Guzhovskii, Atomnaya Energiya 12 (62) 5.
304. Ciric et al., Fizika (Yugoslavia) 7, Suppl. 1 (77) 39.
305. Subotic et al., Fizika (Yugoslavia) 9, Suppl. 1 (77) 44.
306. Fowler, Caughlan and Zimmerman, Ann. Rev. Astro. & Astrophys. 13 (75) 69.
307. Middlton and Pullen, Nucl. Phys. 51 (64) 50.
308. Hunchen et al., Nucl. Phys. 58 (64) 417.
309. Jelley et al., Phys. Rev. C11 (75) 2049.
310. Hardekopf, Bull. Am. Phys. Soc. 21 (76) 551.
311. Scheklinski et al., Nucl. Phys. A153 (70) 97.
312. Paul et al., Phys. Rev. 137 (65) B493.
313. Ling, et al., Nucl. Phys. A108 (68) 221.
314. Ling and Blatt, Nucl. Phys. A174 (71) 375.
315. Lin and Chin, J. Phys. (Taiwan) 10 (72) 76.
316. Cocke, Nucl. Phys. A110 (68) 321.
317. Din and Weil, Nucl. Phys. 86 (66) 509.
318. Dixon and Edge, Nucl. Phys. A156 (70) 33.
319. Dixon, Thesis, U. South Carolina (70).
320. Duggan et al., Nucl. Phys. 46 (63) 336.
321. Serov and Guzhovskii, Atomnaya Energiya 12 (62) 5.
322. Stanojevic et al., Fizika 3 (71) 99.
323. Sanada et al., J. Phys. Soc. Japan 26 (69) 853.
324. Wolicki and Meyer, Bull. Am. Phys. Soc. 6 (61) 415.
325. Orihara et al., Nucl. Phys. A139 (69) 226.
326. Cusson, Nucl. Phys. 86 (66) 481.
327. Bingham, Thesis, Florida State U. (70).
328. Bingham et al., Nucl. Phys. A175 (71) 374.
329. Bohler et al., Nucl. Phys. A179 (72) 504.
330. Kelleter et al., Nucl. Phys. A210 (73) 502.
331. Spear, Australian J. Phys. 12 (59) 99.
332. Kavanagh, Nucl. Phys. 18 (60) 492.
333. Mashkarov et al., Izv, Akad. Nauk SSSR (Ser. Fiz.) 37 (73) 1729.
334. Kiss, et al., Nucl. Phys. A282 (77) 44.
335. Kild and Crinean, Australian J. Phys. 27 (74)663.
336. Yasue et al., J. Phys. Soc. Japan 36 (74) 1254.
337. Dearnaley, Phil. Mag. 1 (56) 821.
338. Mozer, Phys. Rev. 104 (56) 1386.
339. Mo and Hornyak, Phys. Rev. 187 (69) 1220.
340. Rohrer and Brown, Nucl. Phys. A210 (73) 465.

341. Bertrand et al., Comm. A L'energie Atomique, RPT. CEA 3575 (68).
342. Montague et al., Nucl. Phys. A199 (73) 457.
343. Sierk and Tombrello, Nucl. Phys. A210 (73) 341.
344. Tu and Hornyak, Bull. Am. Phys. Soc. 14 (69) 489
345. Votava, Thesis, U. North Carolina (72).
346. Djaloeis et al., Nucl. Phys. 15 (72) 266.
347. Powell et al., Nucl. Phys. A147 (70) 65.
348. Lombard and Friedland, Z. Phys. 249 (72) 349.
349. Machali et al., Nucl. Phys. A112 (68) 654.
350. Renken, Phys. Rev. 132 (63) 2627.
351. Ralph and Dunnam, Phys. Rev. 120 (60) 249A.
352. Bardes and Owen, Phys. Rev. 120 (60) 1369.
353. Evans et al., Phys. Rev. 75 (49) 1161.
354. Kotlay, Acta. Phys. Acad. Sci. Hung. 16 (63)93.
355. Siemssen et al., Nucl. Phys. 69 (65) 209.
356. Canavan, Phys. Rev. 87 (52) 136.
357. Biggerstaff et al., Nucl. Phys. 36 (62) 631.
358. De Jong et al., Physica 18 (52) 676.
359. Dolinov and Melikov, Vest. Mosk. Univ. Fiz. Astron., P116 (66).
360. Ambrossino et al., J. Physique C1 (66) 62.
361. Farouk et al., Z. F. Phys. 201 (67) 52.
362. Juric, Phys. Rev. 98 (55) 85.
363. McCrary et al., Phys. Rev. 108 (57) 392.
364. Read and Calvert, Proc. Phys. Soc. 77 (61) 65.
365. Read et al., Nucl. Phys. 23 (61) 386.
366. Bondouk et al., Ann. Der. Phys. 32 (75) 255.
367. Friedland et al., Z. Phys. 267 (74) 97.
368. Sledzinska et al., Acta. Phys. Polonica 88 (77) 277.
369. Tanaka, J. Phys. Soc. Japan 44 (78) 1405.
370. Zwieglinski et al., Nucl. Phys. A250 (75) 93.
371. Cohen and Herling, Nucl. Phys. A141 (70) 595.
372. Nam and Osetinskii, Soviet J. Nucl. Phys. 9 (69) 279.
373. Earwaker, Nucl. Phys. A90 (67) 56.
374. Bondouk et al., Rev. Roumaine Phys. 19 (74) 653.
375. McEver et al., Nucl. Phys. A178 (72) 529.
376. Taylor et al., Nucl. Phys. 15 (72) 31.
377. Artemov et al., Yadernaya Fiz. 1 (65) 1019.
378. Dorenbusch and Browne, Phys. Rev. 131 (63) 1212.
379. Ehlers, Thesis, Washington State U. (70).
380. Moazed and Holmgren, Phys. Rev. 166 (68) 977.
381. Goss, Thesis, Ohio State U. (70).
382. Goss et al., Phys. Rev. C7 (73) 1837.
383. Taylor et al., Nucl. Phys. 65 (65) 318.
384. Saleh, et al., Ann. Der Physik 31 (74) 76.
385. Overley, Thesis, Caltech (60).
386. Overley and Wahling, Phys. Rev. 128 (62) 315.
387. Boerli et al., Fizika (Yugolsavia) 2 (70) 19.
388. Jenkin et al., Nucl. Phys. 50 (64) 516.
389. Segel et al., Phys. Rev. 145 (66) 736.
390. Szabo et al., Nucl. Phys. A195 (72) 527.

CHAPTER II

REFERENCES

1. Taschek, Phys. Rev. 61 (42) 13.
2. Sherr et al., Phys. Rev 72 (47) 662.
3. Kocher and Clegg, Nucl. Phys. A132 (69) 455.
4. Wilson et al., Nucl. Phys. A130 (69) 624.
5. Kikuchi et al., J. Phys. Soc. Japan 15 (60) 9.
6. Kerman, Phys. Rev. 107 (57) 200.
7. Kiceleva et al., Ukr. Fiz. Zh. 4 (71) 83.
8. Cahill et al., Phys. Rev C4 (71) 83.
9. Cadlwell and Richardson, Phys. Rev. 98 (55) 28.
10. Allred and Rosen, Phys. Rev. 79 (50) 227.
11. Karr et al., Phys. Rev. 81 (51) 37, 78 (50) 292.
12. Allred et al., Phys. Rev. 88 (52) 433.
13. Simpson, Thesis, Rice Univ., Houston (65).
14. Grötzschel et al., Nucl. Phys. A176 (71) 261.
15. Brolley Jr. et al., Phys. Rev. 117 (60) 1307.
16. Mather, Phys. Rev. 88 (52) 1408.
17. Heither et al., Proc. Roy. Soc. A190 (47) 180.
18. Brown et al., Phys. Rev. 88 (52) 253.
19. Tuve et al., Phys. Rev. 50 (36) 806.
20. Bunker et al., Nucl. Phys. A113 (68) 461.
21. Balashko et al., Zh. eksp. Teor. Fiz. 36 (59) 1937, JETP (soviet Physics) 9 (59) 1378.
22. Baumann, J. Phys. Rad. 18 (57) 337.
23. Jarmie et al., Phys. Rev. 130 (63) 1987.
24. Balashko et al., JETP 19 (64) 1281.
25. Kurepin, Trudy of the Lebedev Phys. Inst., Vol. 33 (65) p.1 (Transl. by Consultant Bureau, N.Y. 66).
26. Jarmie and Allen, Phys. Rev. 114 (59) 176.
27. Hemmendinger et al., Phys. Rev. 79 (49) 1137.
28. Ennis and Hemmendinger, Phys. Rev. 95 (54) 772.
29. Brolley et al., Phys. Rev. 117 (60) 1307.
30. Classen et al., Phys. Rev. 82 (51) 589.
31. Seagrave, Proc. Conf. on Nuclear Forces and the Few Nuclear Problem, London (59) Vol. II, p.583.
32. Macklin and Gibbons, EANDC-50-S, Vol. I (65).
33. Willard et al., Phys. Rev. 90 (53) 865.
34. Jarmie and Seagrave LA-2014 (56).
35. Gibbons and Macklin, Phys. Rev. 114 (59) 571.
36. Batchelor et al., Rev. Sci. Instr. 26 (55) 1037.
37. Costello et al., Nucl. Sci. Eng. 39 (70) 409.
38. Vlasov et al., JETP 1 (55) 500.
39. Coon, Phys. Rev. 80 (50) 488.
40. Sayres et al., Phys. REv. 122 (61) 1853.

441. Chase et al., Phys. Rev. 166 (68) 997.
442. Williams et al., Phys. Rev. 144 (66) 801.
443. Olness and Warburton, Phys. Rev. 166 (68) 1004.
444. Buechner et al., Phys. Rev. 79 (50) 262.
445. Elkin, Phys. Rev. 92 (53) 127.
446. Fortune and Vincent, Phys. Rev. 185 (69) 1401.
447. Friedland and Verleger, Z. Phys. 222 (69) 138.
448. Breuer, Z. Phys. 178 (64) 268.
449. Kavanagh and Barnes, Phys. Rev. 112 (58) 503.
450. Weller and Blue, Nucl. Phys. A211 (73) 221.
451. Din et al., Nucl. Phys. A93 (67) 190.
452. Almond and Risser, Nucl. Phys. 72 (65) 436.
453. Thornton et al., Nucl. Phys. A198 (72) 397.
454. Silverstein and Herling, Phys. Rev. 181 (69) 1512.
455. Ciric et al., Fizika (Yugoslavia) 9, Suppl. 1 (77) 39.
456. Black et al., Nucl. Phys. A153 (70) 233.
457. Holmgren et al., Phys. Rev. 114 (59) 1281.
458. Hahn and Ricci, Nucl. Phys. A101 (67) 353.
459. Mante et al., Paper 8B6, Asilomar (73).
460. Brill, Soviet J. Nucl. Phys. 1 (65) 37.
461. Liskien and Paulsen, Report EANDC (E) - 143 "L" (72).
462. Liskien and Paulsen, Report EANDC (E) - 152 "L" (72).
463. Liskien and Paulsen, Report EANDC (E) - 144 "L" (72).
464. G. M. Hale and D. C. Dodder, "R-Matrix Analysis of Light-Element Reactions for Fusion Applications", Presented at the International Conference on Nuclear Cross Sections for Technology, Knoxville, TN, Oct. 79.
465. A. Elwyn et al., private communication.

*179. Hemmendinger, Bull. Am. Phys. Soc. 1 (56) 96.

III. Theory

The proper determination of the potential of an advanced fuel cycle requires a study of fusion reaction kinetics, including subtle effects like fast fusion, nuclear elastic and inelastic scattering, Doppler broadening of the energy distribution of reaction products, and the partition of slowing down energy between ions and electrons. The next sections discuss these effects in detail.

1. Slowing Down Theory

A typical fusion plasma temperature is in the tens to hundreds of keV range, while the reaction products are in the MeV to tens of MeV range. To treat the relaxation of the reaction products, the rate of energy loss of a charged particle by coulomb scattering has been calculated numerous times with varying degrees of sophistication.[1-4] It is necessary to take into account, for light elements, the nuclear-force contribution to scattering. This has also been noted by Devanly and Stein.[5] However, these previous studies[1-5] assumed that charged particle slowing down can be described by a continuous theory. This approximation is valid only if the particle energy transfer per collision is small. However, nuclear elastic scattering, large angle coulomb scattering, nuclear inelastic scattering and fast fusion reactions will transfer large amounts of energy which cannot be properly described by the continuous slowing down theory. A better treatment of the process is to use a continuous theory for the small energy

transfer range and a discrete theory for the large energy transfer range.

The small energy transfer collisions due to coulomb scattering are typically several orders of magnitude larger than other nuclear reaction cross sections at small angle. However, in some cases, nuclear-coulomb interference could be on the same order. It is assumed that coulomb scattering and nuclear-coulomb interference are the only sources of small energy transfer collisions. With adjustments which will be described later, coulomb scattering interactions can properly describe the slowing down time based on small energy transfer collisions.

The average instantaneous rate of coulomb energy loss for a particle, k, slowing down in a plasma consisting of several kinds of particles j, can be expressed by the following two equations:[2,6]

$$-\left(\frac{\partial E_k}{\partial t}\right)_e^c = \left(\frac{4\pi e^4}{m_e}\right)\left(\frac{Z_k^2}{v_k}\right) n_i L_e F\left(\frac{v_k}{u_e}\right) \bar{Z} \tag{59}$$

$$-\left(\frac{\partial E_k}{\partial t}\right)_i^c = \left(\frac{4\pi e^4}{m_e}\right)\left(\frac{Z_k^2}{v_k}\right) n_i m_e \sum_{\ell} \frac{Z_\ell^2 \beta_\ell L_\ell F(v_k/u_\ell)}{m_\ell} \tag{60}$$

where the superscript c refers to coulomb scattering and the subscripts e, k and ℓ refer to electron, particle k and ion species ℓ. Further, Z refers to charge number, m to atomic mass (a.m.u.), n_i to total ion density, β to the atomic fraction of ions in the plasma and u to the speed of the thermal particle. The subscript j refers

to either electron or ions and $x_j \equiv v_k/u_j$.

$$F(x_j) \equiv \mathrm{erf}(x_j) - (1 - m_j/m_k)\, x_j\, e^{-x_j^2} \qquad (61)$$

The coulomb logarithm, L_j, is written as

$$L_j = \frac{1}{2}\, \ell n(1 + \Lambda_j^2) \quad , \qquad (62)$$

where the argument is given by the following ratio:

$$\Lambda_j = \ell_D/b_{oj} \quad \text{classical} \qquad (63)$$

$$= \ell_D/\lambda_j \quad \text{quantum} \qquad (64)$$

with ℓ_D, b_{oj} and λ_j being the total Debye shielding length, the cutoff impact parameter and the center of mass wavelength in two body scattering, respectively.

By adjusting the cutoff impact parameter b_{oj} so that only small energy transfer collisions can occur and by adding a weighting factor to take the nuclear-coulomb interference contribution into account, the continuous slowing down theory can be described by:

$$-\left(\frac{\partial E_k}{\partial t}\right)_e^S = \left(\frac{4\pi e^4}{m_e}\right)\left(\frac{Z_k^2}{v_k}\right) n_i\, L_e\, F(v_k/u_e)\, \bar{Z} \qquad (65)$$

$$-\left(\frac{\partial E_k}{\partial t}\right)_i^S = \left(\frac{4\pi e^4}{m_e}\right)\left(\frac{Z_k^2}{v_k}\right) n_i\, m_e \sum_{\ell} \frac{Z_\ell^2 \beta_\ell\, L_\ell^*\, W_\ell F(v_k/u_\ell)}{m_\ell} \qquad (66)$$

where the superscript S refers to small energy transfer scattering, L_ℓ^* is the adjusted value of L_ℓ (called small energy transfer

logarithm), and W refers to the weighting factor which takes the nuclear-coulomb interference contribution into account. Define

$$L_\ell^* = L_\ell \cdot \ell n \left(\frac{1-\cos\theta_c}{1-\cos\theta_b}\right) / \ell n \left(\frac{1-\cos\theta_b}{1-\cos\theta_d}\right) \tag{67}$$

$$W_\ell = \int_{\cos\theta_d}^{\cos\theta_c} \frac{d\sigma^S}{d\Omega} \, d\cos\theta \Big/ \int_{\cos\theta_d}^{\cos\theta_c} \frac{d\sigma^C}{d\Omega} \, d\cos\theta \tag{68}$$

where θ_d refers to the deflection angle (in C.M. system) corresponding to an impact parameter of ℓ_D, θ_b is the cutoff angle for traditional coulomb scattering, and θ_c is the deflection angle for maximum energy transfer in the small energy transfer range.

Summing the two contributions, i.e., Eqs. (65) and (66), and making the substitutions $E_k = \frac{1}{2} m_k v_k^2$, $ds = v_k \, dt$, the energy loss becomes related to the path length by:

$$-n_i \, ds = dv_k [G(v_k, t)]^{-1} \tag{69}$$

where:

$$G(v_k) = \left(\frac{4\pi e^4}{m_e}\right)\left(\frac{Z_k}{m_k v_k^3}\right)\left[L_e \, F(v_k/u_e)\bar{Z} + m_e \sum_\ell \frac{Z_\ell^2 \beta_\ell \, L_\ell^* \, W_\ell \, F(v_k/u_\ell)}{m_\ell}\right] . \tag{70}$$

Since the composition and the temperature may change with time, e.g., reactions are taking place in the plasma, the function G is time-

dependent and denoted as G(v,t).

2. Reactions while slowing down

If a slowing down particle k can react with a background particle ℓ, with a cross section $\sigma^R_{k\ell}$, then the instantaneous probability per unit length that the reaction will take place during the slowing down process is given by:

$$\frac{dP^{*R}_{k\ell}(v_k,t)}{dS} = \frac{1}{v_k}\int d\vec{v}\ \sigma^R_{k\ell}(|\vec{v}_k-\vec{v}|)\ |\vec{v}_k-\vec{v}|f_\ell(v,t) \qquad (71)$$

where $f_\ell(v,t)$ is the distribution function of particle ℓ and the superscript (*) denotes an instantaneous quantity. The instantaneous reaction probability of a particle k about its velocity v_k can be expressed as

$$P^{*R}_{k\ell}(v_k,t)\ dv_k = \left[\int d\vec{v}\ \frac{f_\ell(v,t)\ \sigma_{k\ell}(|\vec{v}_k-\vec{v}|)\ |\vec{v}_k-\vec{v}|}{v_k\ n_i\ G(v_k,t)}\right] dv_k \qquad (72)$$

The integration over the slowing down path can be converted to an integration from the initial velocity v_k to the final velocity u_k, yielding:

$$P^R_{k\ell}(v_k \to u_k,t) = \int_{u_k}^{v_k} d\vec{V}\int d\vec{v}\ \frac{f_\ell(v,t)\ \sigma^R_{k\ell}(|\vec{V}-\vec{v}|)|\vec{V}-\vec{v}|}{V\ n_i\ G(V,t)} \qquad (73)$$

Since the particle k can react with one or more ions or react through several channels the total reaction probability is given as a sum

over all reactions and channels. The instantaneous probability then becomes:

$$P^{*R}_{kT}(v_k,t)\,dv_k = \{\sum_{\ell}\int d\vec{v}\,\frac{f_\ell(v,t)[\sum_n \sigma^{Rn}_{k\ell}(|\vec{V}-\vec{v}|)]|\vec{V}-\vec{v}|}{v_k\, n_i\, G(v_k,t)}\}\,dv_k \qquad (74)$$

and

$$P^{R}_{kT}(v_k \rightarrow u_k,t) = \sum_{\ell}\int_{u_k}^{v_k} d\vec{V}\int d\vec{v}\,\frac{f_\ell(v,t)[\sum_n \sigma^{Rn}_{k\ell}(|\vec{V}-\vec{v}|)]|\vec{V}-\vec{v}|}{V\, n_i\, G(V,t)} \qquad (75)$$

The time-evolution of the full velocity distribution function of the various ions can be calculated by the expensive non-linear Fokker-Plank method. However, a linear approximation, the multigroup energy technique, will provide an inexpensive solution for the reaction kinetics study. It is assumed that the velocity distribution function is made up of a Maxwellian bulk with a small tail of energetic particles and can be expressed as:

$$f_\ell(v,t) = f^M_\ell(v,t) + f^*_\ell(v,t)$$

where f_ℓ, f^M_ℓ and f^*_ℓ refer to the distribution function, the Maxwellian distribution function and the stripped distribution function which represents the tail of energetic particles. The discrete nature of large energy transfer events such as nuclear elastic scattering, large angle coulomb scattering, nuclear inelastic scattering and fast fusion reactions can also be fit into this scheme conveniently.

3. The reactivity of a propagating reaction

The reactivity can be enhanced by the propagating effect in the cycles such as p-^{6}Li. The p-^{6}Li cycle is particularly useful to demonstrate the procedure to derive the power density formula for a propagating reaction cycle.

In order to show the procedures for which the power density formula of a fully propagating reaction cycle is obtained, an overly simplified case is to consider the reactions

$$p + {}^6Li \rightarrow {}^3\bar{\bar{H}}e + \alpha \qquad (76)$$

$$^3He + {}^6Li \rightarrow \bar{\bar{p}} + 2\alpha \qquad (77)$$

The Maxwellian fusion reaction rates in this case are

$$a_{16} = n_1 n_6 \langle\sigma v\rangle_{16} \qquad (78)$$

$$a_{36} = n_3 n_6 \langle\sigma v\rangle_{36} \qquad (79)$$

where n_1, n_3 and n_6 are the densities of protons, ^{3}He, and ^{6}Li respectively, and $\langle\sigma v\rangle$'s are the reaction rate parameters. Let $\bar{\bar{\Gamma}}_{36}$, $\bar{\bar{\Gamma}}_{16}$ be the probabilities that fast ^{3}He and fast protons produced by reactions(76) and (77) will fuse with ^{6}Li prior to slowing down. Then the total production rate of ^{3}He is

$$P_3 = \frac{a_{16} + a_{36}\bar{\bar{\Gamma}}_{16}}{1 - \bar{\bar{\Gamma}}_{36}\bar{\bar{\Gamma}}_{16}} \qquad (80)$$

The power output in this branch is $P_3 Q_{16}$. The consumption rate of ^{3}He is

$$C_3 = \frac{a_{36} + a_{16}\bar{\bar{\Gamma}}_{36}}{1 - \bar{\bar{\Gamma}}_{36}\bar{\bar{\Gamma}}_{16}} \qquad (81)$$

The power output in this branch is $C_3 Q_{36}$, where Q_{16} and Q_{36} are the nuclear reaction Q values for reactions (76) and (77)

The equilibrium ^3He content is found by setting $P_3 = C_3$ and gives

$$n_3 = n_1 \frac{\langle\sigma v\rangle_{16}}{\langle\sigma v\rangle_{36}} \frac{(1-\bar{\bar{\Gamma}}_{36})}{(1-\bar{\bar{\Gamma}}_{16})} \qquad (82)$$

By substituting n_3 into the sum of the power output of the two branches, one has the total fusion power density:

$$P_F = a_{16} \frac{(Q_{16}+Q_{36})}{1 - \bar{\bar{\Gamma}}_{16}} \qquad (83)$$

The fusion power density formula in this case is composed of two parts. The numerator is the power density formula of the conventional catalyzed p-^6Li cycle. The denominator expresses the propagating effect.

The power density formula for the more general case with reactions

$$\begin{aligned}
&p + {}^6Li \rightarrow {}^3\bar{\bar{H}}e\ (2.3\ MeV) + \alpha \\
&{}^3He + {}^6Li \rightarrow \bar{\bar{p}}(11.2 MeV) + 2\alpha \\
&D + {}^3He \rightarrow \bar{\bar{p}}(14.6\ MeV) + \alpha \\
&D + D \rightarrow n + {}^3\bar{H}e(.9\ MeV) \\
&D + D \rightarrow \bar{p}\ (3MeV) + T \\
&{}^3He + {}^3He \rightarrow 2\bar{p}\ (3.1\ MeV) + \alpha
\end{aligned} \qquad (84)$$

is complicated. To distinguish fast protons, we have used different numbers of overbars as in eqn.(84) The following notation is used in the power density formula to follow. The probability of fast particles, $\bar{a}$, $\bar{\bar{a}}$, etc. reacting with a thermal particle b is expressed as $\bar{\Gamma}_{ab}$, $\bar{\bar{\Gamma}}_{ab}$, etc. respectively. The Maxwellian reaction rate is expressed as $a_{\ell bc}$, where ℓ denotes the branch the reaction takes. $Q_{\ell bc}$ is the reaction Q value. We find for the fusion power density,

$$P_F = \frac{a_{16} + a_{T22}\bar{\Gamma}_{16} + 2(a_{33}+a_{322}\bar{\Gamma}_{33})\,16 + (a_{36}+a_{322}\bar{\bar{\Gamma}}_{36})\,16 + a_{23}\bar{\bar{\bar{\Gamma}}}_{16}}{1 - (\bar{\Gamma}_{33}\bar{\Gamma}_{16} + \bar{\Gamma}_{36}\bar{\bar{\Gamma}}_{15} + \bar{\Gamma}_{32}\bar{\bar{\bar{\Gamma}}}_{16})} Q_{16}$$

$$+ \frac{a_{36} + a_{16}\bar{\Gamma}_{36} + a_{322}\bar{\bar{\Gamma}}_{36}}{1 - (\bar{\Gamma}_{33}\bar{\Gamma}_{16} + \bar{\Gamma}_{36}\bar{\bar{\Gamma}}_{16} + \bar{\Gamma}_{32}\bar{\bar{\bar{\Gamma}}}_{16})} Q_{36} + \frac{a_{33} + a_{16}\bar{\Gamma}_{33} + a_{322}\bar{\bar{\Gamma}}_{33}}{1 - (\bar{\Gamma}_{33}\bar{\Gamma}_{16} + \bar{\Gamma}_{36}\bar{\bar{\Gamma}}_{16} + \bar{\Gamma}_{32}\bar{\bar{\bar{\Gamma}}}_{16})} Q_{33}$$

$$+ \frac{a_{23} + a_{16}\bar{\Gamma}_{32} + a_{322}\bar{\bar{\Gamma}}_{32}}{1 - (\bar{\Gamma}_{33}\bar{\Gamma}_{16} + \bar{\Gamma}_{36}\bar{\bar{\Gamma}}_{16} + \bar{\Gamma}_{32}\bar{\bar{\bar{\Gamma}}}_{16})} Q_{23} + a_{322}Q_{322} + a_{T22}Q_{T22} \quad . \qquad (85)$$

The density of ^{3}He and of D, as well as the fast fusion probabilities, must be calculated in a self-consistent way.

From the partial balance equations, which take into account all the reactions involved, one can solve for the equilibrium density ratio of species in a fuel cycle. In addition, the energy balance equations and the fast fusion probabilities are needed if the fast reaction events are included. The p-^{6}Li fuel cycle is chosen to illustrate the problems involved and the method developed.

The particle balance equations are cumbersome and it is convenient to use the following notations

$$S_{cab} \equiv \langle cab \rangle \equiv \langle \sigma v \rangle^{c}_{ab} \qquad (\text{in cm}^3/\text{sec})$$

= Reaction parameter for reaction a + b → c + d

where c is a reaction product chosen to characterize the reaction branch (channel)

$S_{ab} \equiv \langle ab \rangle \equiv \sum_i \langle c_i ab \rangle$ includes all of the branches

$G_a \equiv \gamma_a = \frac{n_a}{n_s}$ = the ratio of the number density of specie a to the reference specie s.

$GS_{cab} \equiv (abcab) = \gamma_a \gamma_b 2^{-\delta_{ab}} \langle cab \rangle$ where δ_{ab} is the Kronecker delta.

$GS_{ab} \equiv (ab\ ab) = \gamma_a \gamma_b 2^{-\delta_{ab}} \sum_i \langle c_i ab \rangle$

$GFS_{cab} \equiv (\overline{abcab}) = GS_{cab}$ + all of the fast reactions due to the

$\equiv GS_{cab} + FS_{cab}$ energetic a or b produced in the reactions involved prior to slowing down.

$GFS_{ab} \equiv (\overline{ab\ ab}) = \sum_i (abc_i ab)$.

For p-^{6}Li, the proton is chosen as the reference specie and we define the density ratios as $\gamma_1 = \frac{n_p}{n_p} = 1$, $\gamma_2 = \frac{n_d}{n_p}$, $\gamma_3 = \frac{n_3}{n_p}$, $\gamma_T = \frac{n_T}{n_p}$, $\gamma_6 = \frac{n_6}{n_p}$, $\gamma_L = \frac{n_{7_{Li}}}{n_p}$, $\gamma_7 = \frac{n_{7_{Be}}}{n_p}$. The ion temperature T_i and γ_6 will be specified in each run. The reaction rates of the major reactions considered are denoted by:

$(\overline{26726})$, $(\overline{26L26})$, $(\overline{26T26})$, $(\overline{26326})$, $(\overline{26A26})$, $(\overline{22322})$, $(\overline{22T22})$, $(\overline{16316})$, $(\overline{23P23})$, $(\overline{36236})$, $(\overline{36P36})$, $(\overline{33P33})$, $(\overline{37P37})$, $(\overline{T7PT7})$, $(\overline{27P27})$, $(\overline{TTATT})$, $(\overline{2TA2T})$, $(\overline{2LN2L})$, $(\overline{T32T3})$, $(\overline{T31T3})$, $(\overline{T3PT3})$, $(\overline{TLNTL})$, $(\overline{3LP3L})$, $(\overline{1L71L})$, $(\overline{1LA1L})$, and $(\overline{1T31T})$.

The particle balance equations can be described as follows:

for ^{3}He: $(\overline{26326}) + (\overline{22322}) + (\overline{16316}) + (\overline{1T31T})$

$= (\overline{23\ 23}) + (\overline{36\ 36}) + 2(\overline{33\ 33}) + (\overline{T3\ T3}) + (\overline{37\ 37})$

$+ (\overline{3L\ 3L})$

- (86)

for D: $(\overline{36236}) + (\overline{T32T3}) = (\overline{26\ 26}) + 2(\overline{22\ 22}) + (\overline{23\ 23})$

$+ (\overline{27\ 27}) + (\overline{2T\ 2T}) + (\overline{2L\ 2L})$

- (87)

For ^{7}Be: $(\overline{26726}) + (\overline{36236}) + (\overline{1L71L}) = (\overline{27\ 27}) + (\overline{37\ 37}) + (\overline{T7\ T7})$

- (88)

For T: $(\overline{26T26}) + (\overline{22T22}) = (\overline{T7\ T7}) + 2(\overline{TT\ TT}) + (\overline{2T\ 2T})$

$+ (\overline{T3\ T3}) + (\overline{TL\ TL}) + (\overline{1T\ 1T})$

- (89)

For ^{7}Li: $(\overline{26L26}) = (\overline{2L\ 2L}) + (\overline{TL\ TL}) + (\overline{3L\ 3L}) + (\overline{1L\ 1L})$

- (90)

Although equations (86),(87),(88),(89) and (90) are coupled, the five unknowns (γ_3, γ_2, γ_T, γ_7 and γ_L) can be obtained from the five equations for any T_i provided that the fast reaction rates are known. To calculate the fast reaction probabilities, it is necessary to know all γ values and the electron temperature. To calculate T_e, one must have all γ values, all fast reaction rates, and T_e itself. A self-consistent iteration method is developed to handle the task.

The self-consistent iteration method is a numerical approach to solve for the various γ values, all fast reaction rates, and T_e self-consistently. It consists of 2 inner iteration loops inside a master iteration loop. The calculation is described briefly in the block diagram in Fig. 11.

The character of the energy transfer insures the convergence of the iteration loop which yields T_e and the fast fusion probabilities. However, knowledge of reaction kinetics is required to insure the convergence of other inner iteration loops and the master loop. By design, only a few specific physical parameters are inputs. For example, T_i and γ_6 are the only inputs required for the p-^{6}Li case. The code first prepares all values of S_{cab}

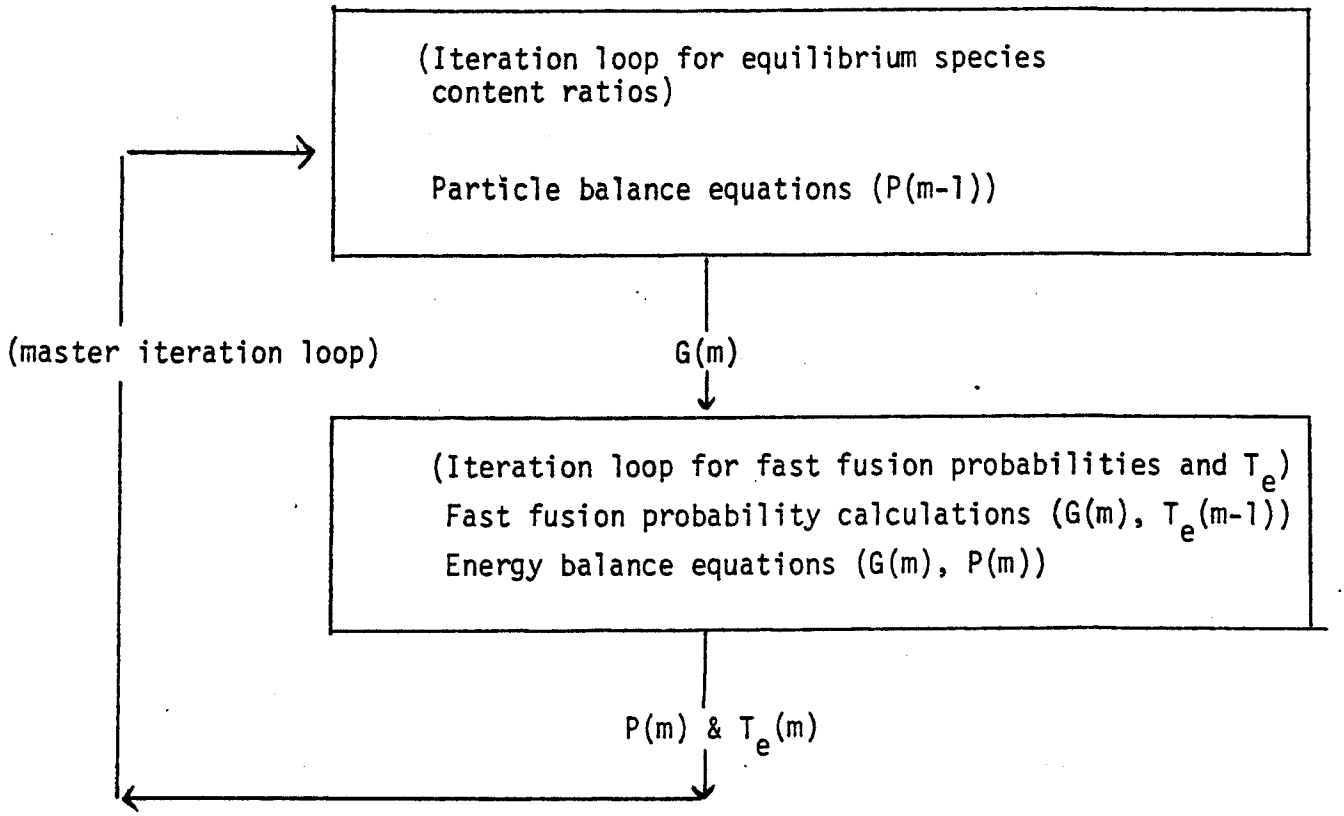

1. Use the fast fusion probabilities of the previous generation (denoted as P(m-1)) in the particle balance equations, iterate and obtain a new generation equilibrium species content ratio (denoted as G(m)).

2. Use G(m) and T_e of the previous generation (denoted as T_e(m-1)) to calculate the fast fusion probabilities. Use G(m) and the fast fusion probabilities in the energy balance equations to calculate T_e. The iteration will yield a new generation value of P(m) and T_e(m).

3. Continue (1) and (2) until G, P, and T_e converge to the degree specified.

Fig. 11

for a given T_i, sets all of the fast reaction probabilities and γ's (except $\gamma_1 = 1$ and γ_6) equal to zero and sets $T_e = .75\ T_i$. The remaining first generation γ's are then calculated based on the above values. The calculations continue according to the procedure outlined and yield consistent values of the equilibrium species content ratios, fast reaction probabilities, and the electron temperature.

4. Energy balance

The ion temperature and electron temperature in an advanced fuel cycle fusion plasma may reach 500 keV. The relativistically corrected Bremsstrahlung and electron-ion rethermalization formulas must be used in the energy balance equations.

Bremsstrahlung radiative power is given[7,8] by:

$$P_x = 2.94 \times 10^{-15}\ n_e^{\,2}\ Z_{eff}\ T_e^{\,1/2}(1+\eta)(keV/cm^3\text{-}s) \qquad (91)$$

where

$$Z_{eff} = \sum_j n_j\ Z_j^{\,2}/n_e, \qquad (92)$$

and the sum extends over all ion species. The relativistic correction factor η is

$$\eta = \frac{2T_e}{m_o c^2} + \frac{2}{Z_{eff}}\left(1 - \frac{1}{\left(1 + \frac{T_e}{m_o c^2}\right)^2}\right) \qquad (93)$$

where $m_o c^2$ is the rest mass energy of the electron.

The electron-ion rethermalization power is given by

$$P_{ie} = \frac{3\times10^{-12} n_e}{T_e^{3/2}} \left(\sum_j \frac{n_j Z_j^2}{A_j}\right) (T_i - T_e)\delta \qquad (94)$$

where δ is a relativistic correction factor given by

$$\delta = 1 - 0.3 \frac{T_e}{m_o c^2} \quad . \qquad (95)$$

5. Doppler Broadening and Energy Distribution from Nuclear Reactions

The spread in energy of the fusion reaction products results from the spread in energy of the colliding particles in the center of mass frame and the translation of center of mass of the colliding ion pair. Let the velocity relative to the laboratory frame of two species be $\vec{V}_1$ and $\vec{V}_2$. The total momentum $\vec{P}$ in the laboratory frame is

$$P = m_1\vec{V}_1 + m_2\vec{V}_2 = (m_1 + m_2)\vec{V}_c = (m_3 + m_4)\vec{V}_c \qquad (96)$$

where species 3 and 4 are products of the reaction. $\vec{V}_c$ is the velocity of the center of mass of the reacting pair. Any radiation given off during

the collision or during the compound nucleus state is neglected for the time being.

The energy of the daughter particles (species 3 and 4) in the center of mass frame are related to the energy of initial particles by:

$$E_3^c + E_4^c = E_1^c + E_2^c + Q \equiv E^c + Q = \frac{1}{2}\frac{m_1 m_2}{m_1+m_2}(\vec{V} - \vec{V}_2)^2 + Q \quad (97)$$

where E_j^c is kinetic energy of particle j in the center of mass and Q is the reaction energy. The energy of the fusion products in the center of mass frame are related by the requirement that:

$$P_3^c + P_4^c = 0 = m_3\vec{U}_3 + m_4\vec{U}_4 \quad (98)$$

$$E_3^c = \frac{1}{2} m_3 U_3^2 = \frac{1}{2} m_3 (-\frac{m_4}{m_3}\vec{U}_4)^2$$

$$= \frac{m_4}{m_3} E_4^c \quad (99)$$

Hence the center of mass energy equation gives

$$E_3^c + E_4^c = (1 + \frac{m_3}{m_4}) E_3^c = E^c + Q \quad (100)$$

or

$$E_3^c = \frac{m_4}{m_3+m_4}(E^c + Q) \quad (101)$$

Since the energy of particle 3 in the center of mass frame is

$$E_3^c = \frac{1}{2} m_3 U_3^2 = \frac{m_4}{m_3+m_4}(E_c + Q) \quad , \quad (102)$$

one has

$$U_3 = [\frac{2}{m_3} \cdot \frac{m_4}{m_3+m_4}(E^c + Q)]^{1/2} \quad . \quad (103)$$

Hence, the energy of particle 3 in the laboratory frame will be

$$E_3 = \frac{1}{2} m_3 V_3^2 = \frac{1}{2} m_3 (\vec{V}_c + \vec{U}_3)^2$$

$$= \frac{1}{2} m_3 (U_3^2 + V_c^2 + 2V_c U_3 \cos\theta) - - - \qquad (104)$$

where θ is the angle between $\vec{V}_c$ and $\vec{U}_3$.

The angular distribution of a reaction in the energy range of interest could be isotropic in the center of mass frame (such as for the D-T reaction), or anisotropic (such as for the p-^{6}Li reaction. See Fig. 12.)

We can rewrite equation (104) in terms of the initial state and the final emission angle θ as

$$E_3 = \frac{1}{2} m_3 (U_3^2 + V_c^2 + 2V_c U_3 \cos\theta)$$

$$= \frac{1}{2} m_3 U_3^2 + \frac{1}{2} m_3 \left(\frac{m_1\vec{V}_1 + m_2\vec{V}_2}{m_1 + m_2}\right)^2 + m_3 \left|\frac{m_1\vec{V}_1 + m_2\vec{V}_2}{m_1 + m_2}\right| U_3 \cos\theta$$

$$= \frac{m_4}{m_3+m_4}(E^c+Q) + \frac{m_3}{(m_1+m_2)^2}[m_1E_1+m_2E_2 + 2(m_1m_2E_1E_2)^{1/2}\cos\xi]$$

$$+ \frac{2}{m_1+m_2}[m_1E_1 + m_2E_2 + 2(m_1m_2E_1E_2)^{1/2}\cos\xi]^{1/2}\left[\frac{m_3m_4}{m_3+m_4}(E^c+Q)\right]^{1/2}\cos\theta$$

$$- - - \qquad (105)$$

where ξ is the angle between the velocities $\vec{V}_1$ and $\vec{V}_2$.

The term $\frac{m_4}{m_3+m_4} E^c$ in equation (105) represents an additive contribution that is typically on the order of a few tens of keV's for D-T Maxwellian reactions. It can be on the order of hundreds of keV's for p-^{6}Li Maxwellian

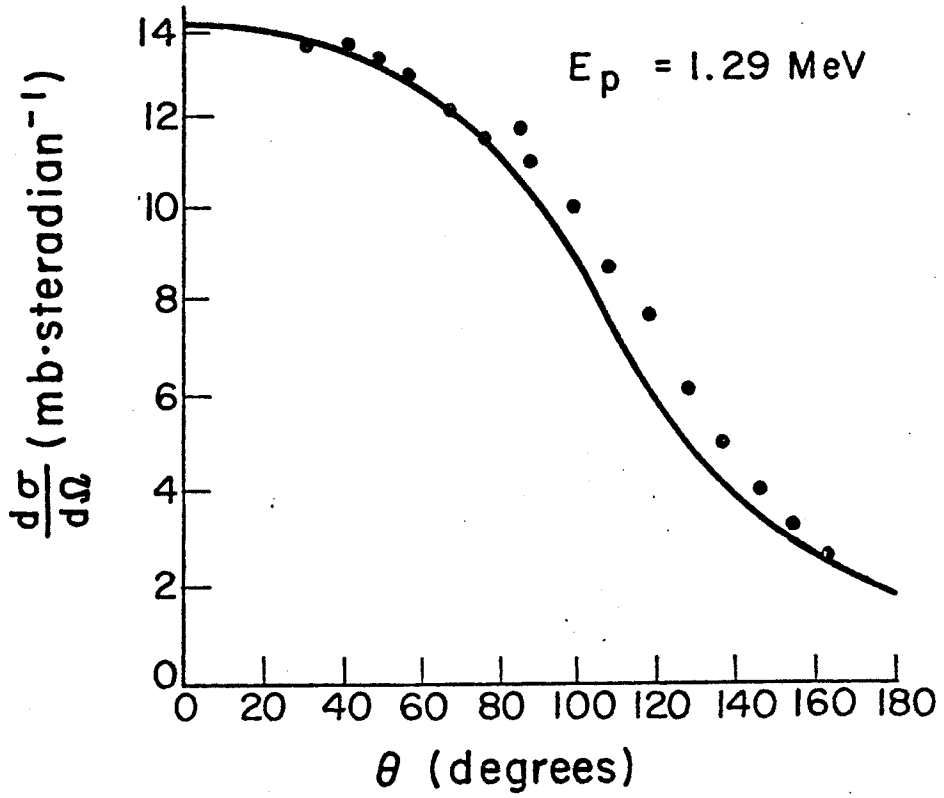

Fig. 12 Angular distribution of the p-^{6}Li reaction cross section

reactions. In addition, the variation of E^c is roughly equal to the width of the reaction cross section. The contribution from the motion of the center of mass,

$$\frac{m_3}{(m_1+m_2)^2}\left[m_1E_1 + m_2E_2 + 2(m_1m_2E_1E_2)^{1/2}\cos\xi\right] \qquad (106)$$

ranges from a few keV to a few hundred keV. The major spread in energy comes from the term

$$\frac{2}{m_1+m_2}\left[m_1E_1 + m_2E_2 + 2(m_1m_2E_1E_2)^{1/2}\cos\xi\right]^{1/2}\left[\frac{m_3m_4}{m_3+m_4}(E^c+Q)\right]^{1/2}\cos\theta \qquad (107)$$

since this term is proportional to the product of the relative velocity of the reaction products and the translational velocity of the center of mass.

If there is radiation given off during the collision or during the compound nucleus state, the energy of particle 3 in the laboratory frame can be expressed as in equation (105)provided that E^c+Q is replaced by $E^c + Q - E_\gamma$, where E_γ is the radiation energy given off.

In order to derive the energy distribution function of the reaction products, let us consider the ion species 1 with number density n_1 and velocity distribution $f_1(\vec{V}_1)$ reacting with ion species 2 with number density n_2 and velocity distribution function $f_2(\vec{V}_2)$. The reaction rate per unit volume for a process with reaction cross section $\sigma(|\vec{V}_1-\vec{V}_2|)$ is

$$R = n_1n_2\int d^3\vec{V}_1 d^3\vec{V}_2 f_1(\vec{V}_1)f_2(\vec{V}_2)|\vec{V}_1 - \vec{V}_2|\sigma(|\vec{V}_1 - \vec{V}_2|) \qquad (108)$$

The energy distribution of the reaction products with mass m_3 and energy E_3 can be expressed as

$$\frac{dR}{dE_3} = n_1 n_2 \int d^3\vec{V}_1 d^3\vec{V}_2 f_1(\vec{V}_1) f_2(\vec{V}_2) \; |\vec{V}_1 - \vec{V}_2| \frac{d\sigma}{dE_3}$$

$$= n_1 n_2 \int d^3\vec{V}_1 d^3\vec{V}_2 f_1(\vec{V}_1) f_2(\vec{V}_2) \; |\vec{V}_1 - \vec{V}_2| \frac{d\sigma}{d\Omega} \frac{d\Omega}{dE_3}$$

$$= n_1 n_2 \int d^3\vec{V}_1 d^3\vec{V}_2 f_1(\vec{V}_1) f_2(\vec{V}_2) \; |\vec{V}_1 - \vec{V}_2| \frac{d\sigma}{d\Omega} \cdot \frac{-d(\cos\sigma) d\phi}{dE_3}$$

$$= 2\pi n_1 n_2 \int d^3\vec{V}_1 d^3\vec{V}_2 f_1(\vec{V}_1) f_2(\vec{V}_2) |\vec{V}_1 - \vec{V}_2| \frac{d\sigma}{d\Omega} \cdot \left(- \frac{d(\cos\theta)}{dE_3}\right) \qquad (109)$$

The term $\frac{d}{dE_3}(\cos\theta)$ can be found from equation (105) and therefore $\frac{dR}{dE_3}$ can be calculated, provided $\frac{d\sigma}{d\Omega}$ is given. Equation(109) can also be used for both elastic and inelastic scattering processes.

CHAPTER III

REFERENCES

1. L. Longmire, Elementary Plasma Physics, Interscience Publishers, New York ('63)
2. I. P. Shkarofsky, T.W. Johnson and M.P. Bachynski, The particle kinetics of plasma, Addison-Wesley Publishing Co., Inc., Reading, Massachusetts ('66)
3. S. T. Butler and M.J. Buckingham, Phys. Rev. 126 ('62) 1
4. D. J. Sigmar and G. Joyce, Nucl. Fusion 11 ('71) 447
5. J. J. Devanly and M.L. Stein, Nucl. Sci and Eng. 46 ('71) 323
6. W. A. Houlberg, UWFDM 103 ('74)
7. J. M. Dawson, UCLA Plasma Group Report PPG-273 ('76)
8. J. G. Cordey, Lecture 2. Course on Theory of Magnetically Confined Plasma (Varenna, Italy) Sept. 1977.

IV. Advanced fuel cycle burn kinetics code

The advanced fusion fuel cycle analysis requires a time dependent burn kinetics code to follow the many reactions that can be involved, including subtle effects like two component fusions, nuclear elastic and inelastic scattering, Doppler broadening of the energy distribution of reaction products, and the fraction of slowing down energy given separately to the ions and electrons. In addition, advanced fuel cycles are likely to operate at ion temperatures approaching 300 keV and electron temperatures in excess of 100 keV. As such, a careful calculation of relativistic bremsstrahlung losses and of synchrotron radiation is required.

The next sections describe existing fusion burn codes and modifications we intend to develop.

1. Overview of the State-of-the-Art

The burn codes developed to date have all been specialized to answer specific questions about the burn dynamics under rather simple burn conditions.

(1) The University of Illinois

Some six different burn codes (Table 6 developed at the University of Illinois are focused[1] on fuels containing D, T and ^{3}He. Most of these codes are designed for the analysis of steady-state burns. Start-up scenarios can be examined using the "start-up code" but here again the scope of reactants is very restricted.

CODE CHECKLIST	Tokamak Global	Bumpy Torus	SAFFIRE (FRM)	A-FLINT (pellet)	Startup (FRM)	Startup (Tokamak)
Fusion Reactions included	Cat D, D-He^3 D-He^3 breeder √	D-T, Cat D D-He^3 √	D-T, D-D, Cat D, D-He^3 √	D-T, all D-D √		Cat D, D-T D-He^3, D-D
Time dependance				√	√	√
Heating and refueling model	√	√	√		√	√
Bremsstrahlung	√		√	√	√	√
Cyclotron	√		√			√
Diffusion & Conduct	√		√		√	√
Energy dep. from fast fusion products:						
Coulomb	√	√	√	√	√	√
Nuclear	√					
Fusion Multip.	√			√		(√)
Applications:						
Burn Dynamics	√			√		√
Spectrum of power	√		√			√
Documentation			√			√
Availability			√			
Running Cost	√	√	√	√	√	√
Documentation						√
& Availability of Results	√		√	√		√
Interest in generating new results	√	√	√		√	

Table 6 - Checklist of Codes, Modelling Fusion Approaches (University of Illinois)

(2) The ECF Code

The ECF Code at Oak Ridge[2] is now capable of handling over 30 different fusion reactions. In handles fusion power multiplication from fast ions and nuclear elastic scattering as linear processes. The relaxation of fast particles by Coulomb or nuclear elastic collisions is treated assuming the background thermal plasma to be stationary during the slowing-down of the fast particles. This is not appropriate in those situations in which the evolution of the plasma parameters is faster than the relaxation times of fast particles. The code is however adequate for establishing the conditions of a mild steady-state thermonuclear burn.

(3) The FOKN Code

The FOKN Code[3,4] developed at LLL, is the only fully non-linear burn code. This code solves for the time-evolution of the full velocity distribution function of the various reactants. The linear approximation, i.e., the assumptions that the velocity distribution function is made up of a Maxwellian bulk with a small tail of energetic particles is dispensed with. The full details of the time-evolution of this distribution are also available which makes possible the exploration of intense thermonuclear burns and rapid start-up scenarios. This code also includes the details of the effects of nuclear elastic collisions, synchrotron radiation and bremsstrahlung on the shapes of the distribution functions.

The major drawbacks of this code are:

The level of its detail makes it very expensive to run.

The reactions associated with lithium and beryllium have not yet been included.

(4) The University of Wisconsin Code

The University of Wisconsin Code[5], a blend of the Oak Ridge ECF and the Livermore FOKN codes, treats all of the reactions included in the ECF code and more. The slowing-down of fast particles is handled by a linear multigroup technique which allows an inexpensive modeling of the time-dependence of fast particle slowing-down processes. At the high energies that fast fusion products normally have, energy diffusion is usually not too important and can be ignored.

(5) Summary

The preceding summary review of existing codes suggests that, for greatest accuracy regardless of price, the most reliable approach to an advanced fuel burn code is to expand the Livermore FOKN code which already includes most of the relevant physical effects but does not yet include reactions involving lithium and beryllium. Such a code would be invaluable in refining the conclusions of simpler and less expensive codes which already include most of the relevant reactants and fusion reactions.

The Oak Ridge ECF Codes are the most appropriate ones for near term exploratory work. Results from this code should be firmed up by an expansion of the University of Wisconsin Code which when completed will be intermediate in physics content between the ECF and the FOKN codes. As noted earlier, such an expanded code will allow a more reliable analysis of fast start-up scenarios at a cost still much smaller than the FOKN Code would allow. The expansion of the Wisconsin Code is proposed in the next section.

2. Outline of the Proposed Advanced Fuel Cycle Burn Kinetics Code

In this section, we describe in some detail the features we intend to develop for inclusion in an advanced fuel cycle burn kinetics code. As part of out present work, several features have already been developed. We will indicate where work has either begun or is completed and where future work is required. To illustrate why various features of the proposed code are required, we will use the $p + {}^6Li$ cycle as the particular example.

Primary Reactions

$$p + {}^6Li \rightarrow {}^3He\ (2.3\ MeV) + {}^4He\ (1.7\ MeV) \quad (110)$$

$${}^3He + {}^6Li \rightarrow p\ (11.3\ MeV) + 2\,{}^4He\ (2.81\ MeV) \quad (111)$$

$$\rightarrow D\ (0.4\ MeV) + {}^7Be\ (0.1\ MeV) \quad (112)$$

$$\rightarrow p + n + {}^7Be \quad (113)$$

Secondary and Tertiary Reactions:

$$D + {}^6Li \begin{cases} \rightarrow n + {}^7Be\ (.42\ MeV) \\ \rightarrow p\ (4.4\ MeV) + {}^7Li\ (.63\ MeV) \\ \rightarrow p\ (1.6\ MeV) + T + {}^4He \\ \rightarrow n + {}^3He + {}^4He \\ \rightarrow 2\,{}^4He\ (11.2\ MeV) \end{cases} \quad (114)$$

$$D + {}^3He \longrightarrow p\ (14.6\ MeV) + {}^3He\ (4.7\ MeV) \quad (115)$$

$$D + D \begin{cases} \rightarrow n + {}^3He\ (.82\ MeV) \\ \rightarrow p\ (3\ MeV) + T\ (1\ MeV) \end{cases} \quad (116)$$

$$D + {}^7Be \longrightarrow p\ (11.2\ MeV) + 2\,{}^4He\ (2.8\ MeV) \quad (117)$$

$$D + T \longrightarrow n + {}^4He\ (3.5\ MeV) \quad (118)$$

$$T + {}^3He \begin{cases} \rightarrow D\ (9.6\ MeV) + {}^4He\ (4.8\ MeV) \\ \rightarrow p + n + {}^4He \end{cases} \quad (119)$$

$${}^3He + {}^3He \longrightarrow 2p\ (5.7\ MeV) + {}^4He\ (1.4\ MeV) \quad (120)$$

$${}^3He + {}^7Be \longrightarrow 2p\ (4.5\ MeV) + 2\,{}^4He\ (1.1\ MeV) \quad (121)$$

$$T + {}^7Be \longrightarrow p\ (4.2\ MeV) + n + 2\,{}^4He\ (1.1\ MeV) \quad (122)$$

$$D + {}^7Li \longrightarrow n + 2\,{}^4He\ (2.521\ MeV) \quad (123)$$

In addition there are least thirteeen $^6Li + {}^6Li$ exothermic reactions which produce all elements from H to ^{12}C and produce neutrons. Many of the fusion reaction products are energetic and may react with elements in the background plasma prior to complete slowing down (fast fusion or two-component fusion events). Including these fast fusion events is crucial, particularly for cycles that are either propagating or chain events. Some important fast fusion reactions in the p-^6Li cycle (the fast particle has a bar over the elements designation) include:

$$\left\{ \begin{array}{l} \bar{p} + {}^6Li \rightarrow {}^3\bar{He} + \alpha \\ {}^3\bar{He} + {}^6Li \rightarrow \bar{p} + 2\alpha \\ \bar{p} + {}^6Li \rightarrow {}^3\bar{He} + \alpha \end{array} \right\} \quad (124) \qquad \left\{ \begin{array}{l} \bar{p} + {}^6Li \rightarrow {}^3\bar{He} + \alpha \\ {}^3\bar{He} + D \rightarrow \bar{p} + \alpha \\ \bar{p} + {}^6Li \rightarrow {}^3\bar{He} + \alpha \end{array} \right\} \quad (125)$$

$$\vdots \qquad\qquad \vdots$$

$$\left\{\begin{array}{l} \bar{P} + {}^6Li \rightarrow {}^3\bar{He} + \alpha \\ {}^3\bar{He} + {}^6Li \rightarrow \bar{D} + {}^7Be \\ \bar{D} + {}^6Li \rightarrow \bar{P} + {}^7Li \\ \bar{P} + {}^6Li \rightarrow {}^3\bar{He} + \alpha \\ \vdots \end{array}\right. \quad (126)$$

$$\left\{\begin{array}{l} \bar{P} + {}^6Li \rightarrow {}^3\bar{He} + \alpha \\ {}^3\bar{He} + {}^6Li \rightarrow \bar{D} + {}^7Be \\ \bar{D} + {}^7Be \rightarrow \bar{P} + 2\alpha \\ \bar{P} + {}^6Li \rightarrow {}^3\bar{He} + \alpha \\ \vdots \end{array}\right. \quad (127)$$

and there are many others. As such, there is a high premium placed on the very efficient numerical approach to the treatment of slowing down of fast fusion products. We have developed such an efficient procedure for implementation in the code.

With so many reactions involved, other subtle issues arise which we should point out. In general, it is difficult, a priori, to establish a criterion for the inclusion or rejection of a particular reaction channel. First, while the values for $\langle\sigma v\rangle$ and Q are known, the density of each specie in the plasma is not known. Thus, the fusion reaction rates are unknown. Second, the temperature may vary widely during a burn, so that almost all reactions may at some time be influential. For an initially self-consistent model, all reactions with comparable $\langle\sigma v\rangle$ or $\langle\sigma v\rangle Q$ values should be incorporated. Only parameter studies at a later time will determine whether specific reactions are important in the simulation process. At that point, those which do not affect the results in a significant way will be eliminated.

Another issue involves the techniques used to handle a problem with so many reaction channels and associated time constants. Two standard approaches are:

(A) Write many small codes, each of which solves a specific, limited problem. This is inconvenient since there may be many combinations of reactions of

interest. This approach makes it difficult to perform parametric studies which are required since the inclusion or deletion of a particular reaction channel requires that a new code be written. The University of Illinois burn code has been of this type.

(B) Write one large code incorporating all possible reaction channels in such a way as to be selective with respect to which reactions are included for a particular case. This approach poses a severe problem with respect to execution speed because the straightforward approach is to set switches in code to include or ignore certain selected reactions. This is usually accomplished by means of costly "if" statements. Since $\geq 10^6$ evaluations may be required per run, the time spent trying to speed-up the code by selecting reactions may actually make running time longer. Because of the execution time associated with "if" statements, the two codes which currently incorporate "all" possible reactions (namely the ECF code at Oak Ridge and the FOKN Code at LLL) calculate each reaction channel without any selection scheme. The exeuction time of these codes can be excessive and they do not easily lend themselves to parametric studies.

A solution being pursued by U.W.-Madison code involves the use of certain compiler characteristics to replace "if" statements. This can lead to a fast flexible code which can be used for both simple problems and the most complex. Using these features of "intelligent compilers", the U.W.-Madison simulation code can be made very general in scope and fast in speed. In addition, the same compiler characteristics facilitate the required parametric studies.

With this background, the general features to be included in such an advanced fuel burn kinetics code will be described in the next section.

(1). Basic Equations of the Point Kinetics Burn Code

The basic equations are the particle balance, the energy balance, the fusion reactions induced by energetic particles, the slowing down of fast particles by Coulomb and nuclear elastic collisions and Doppler broadening effects. Since particles are present with energies from thermal to the initial energy of production, the most efficient approach to handling the dynamics is to employ a multigroup energy technique. This approach has already been implemented in a limited way in the present version of our code.

Particle Balance

The evolution of the density of a given specie j is

$\frac{dn_j}{dt}$ = beam source (if any) + slowing down rate from fast adjacent group
+ production rate from nuclear reactions
- slowing down rate to next adjacent group
- consumption rate in nuclear reactions
- confinement loss

where j = 1, 2, 3, . . . represent, for example, e^-, p, D, T, ^{3}He, α, ^{6}Li, ^{7}Li, ^{7}Be, etc. In this multigroup approach the particle balance is affected by the energy balance detailed next. The fusion production and consumption rates also must be averaged over the energy populations of the other reactants.

Energy Balance

The dominant slowing-down process is by Coulomb scattering and the energy loss rate is given by

$$\frac{dE}{dt} = - (8\pi)^{1/2} \left(\frac{Ze^2}{4\pi\varepsilon_o}\right)^2 \sum_j \frac{Z_j^2 N_j \ln \Lambda_j F(\frac{V}{V_j})}{M_j V_j} \qquad (128)$$

$$F(\frac{V}{V_j}) = \frac{V_j}{V}\left(\int_o^{V/V_j} e^{-t^2}\, dt\right) - \left(1 - \frac{M_j}{M}\right)e^{-V^2/V_j^2} \qquad (129)$$

E, M, A, and V are the energy, mass, atomic number, and speed of the fast particle whereas n_j, T_j, M_j, Z_j and V_j are the density, temperature, mass, atomic number and speed, respectively, of the background plasma specie. Nuclear elastic and inelastic scattering reactions are also important and are included in the multigroup approach as

$$\left.\frac{dn_k}{dt}\right|_{\text{nuclear}} = \text{gain through scattering} - \text{loss through scattering}$$

$$= \sum_j \int_0^{t_j} dt \int_{E_{ko}}^{E_k} dE_f \int_{E_{jo}}^{E_j} n_j V_{kj} \sigma_{kj}(E_i, E_f) dE_i)\, f(E_i)$$

$$- \sum_e \int_o^{t_e} dt \int_{\alpha E_{ko}}^{E_{ko}} f(E_f) dE_f \int n_k V_{ko\ kj}(E_i, E_f) dE_i \qquad (130)$$

As is done in the FOKN code, these scattering terms include multi-dimensional integrals which can be evaluated <u>once</u> as transfer matrices prior to a computational run and tabularized.

The evolution of the temperature of the thermal background is obtained from the equations

$$\frac{d}{dt}\sum_j\left(\frac{3}{2} n_j T_j\right) = \text{heating rate by fast particles (Coulomb and nuclear)} - \text{heat loss to electrons} - \text{confinement losses } \left(\frac{3}{2}\sum \frac{n_j T_j}{\tau_{Ej}}\right) \qquad (131)$$

$$\frac{d}{dt}\left(\frac{3}{2} n_e T_e\right) = \text{heating by fast ions} - \text{confinement losses } \left(\frac{3}{2}\frac{n_e T_e}{\tau_{Ee}}\right) - \text{radiation losses} \qquad (132)$$

At present, radiation losses from the electrons include the standard relativistically correct estimates for bremsstrahlung as well as a crude model of synchrotron radiation losses. The latter is difficult to do accurately but a black body level up to a critical harmonic number should be adequate pending more accurate results of a geometry dependent calculation proposed elsewhere.

(2). Treatment of Fast Fusion Events

The fast charged particles undergo coulomb collisions with the background plasma. The energy of the particle is lost to the cooler target and the expression for the rate of energy loss is given in eqn. (128). Let $\sigma(|\vec{V} - \vec{V}_j|)$ be the reaction cross section for a fast charged particle of velocity $\vec{V}$, on a background plasma specie j of velocity $\vec{V}_j$. Assuming that the background plasma specie j has a velocity distribution $f(\vec{V}_j)$ and that $\int f(\vec{V}_j) d^3\vec{V}_j = 1$, the probability of a fast particle slowing down from $E_{\ell+1}$ to E_ℓ and reacting with plasma specie j is given by:

$$\int_{E_{\ell+1}}^{E_\ell} n_j \int |\vec{V} - \vec{V}_j| \sigma(|\vec{V} - \vec{V}_j|) f(\vec{V}_j) d^3\vec{V}_j \frac{dt}{dE_f} dE_f \quad . \quad . \quad . \qquad (133)$$

where $E_f = \frac{1}{2} M V^2$ and $\frac{dE_f}{dt}$ is the total rate of energy loss of the charged particle via coulomb collisions. The integration of the reaction probability involves the evaluation of $\frac{dE_f}{dt}$ which depends on E_f, n_j, T_i and T_e (especially E_f, n_e and T_e). Therefore, it must be performed at each time step (of the calculation of the density energy balance equations).

A fast particle can undergo any of a large number of different reactions; e.g. $\bar{D} + D \rightarrow n + {}^3He$, $\bar{D} + D \rightarrow P + T$, $\bar{D} + T \rightarrow n + \alpha$, $\bar{D} + {}^3He \rightarrow P + \alpha$, $\bar{D} + {}^6Li \rightarrow 2\alpha$, $\bar{D} + {}^6Li \rightarrow P + T + \alpha$, $\bar{D} + {}^6Li \rightarrow n + {}^3He + \alpha$, $\bar{D} + {}^6Li \rightarrow n + {}^3He + \alpha$, $\bar{D} + {}^6Li \rightarrow P + {}^7Li$, $\bar{D} + {}^6Li \rightarrow n + {}^7Be$, $\bar{D} + {}^7Li$, $\bar{D} + {}^7Be$, etc. Including the fast events is crucial, particularly for cycles that are either propagating or chain events.

For these reasons, it has been thought that an advanced fuel cycle burn kinetic code would be prohibitively expensive if one calculates fast fusion probabilities to the required accuracy. We have developed a method around this difficulty.

The reaction probability is

$$\text{Reaction probability for particle slowing down from } E_{\ell+1} \to E_\ell = \int_{E_{\ell+1}}^{E_\ell} n_j \int |\vec{V}-\vec{V}_j| \sigma(|\vec{V}-\vec{V}_j|) f(\vec{V}_j) d^3\vec{V}_j \frac{dt}{dE_f} \cdot dE_f$$

$$\cong n_j \sum_{k=1}^{K} \left[\int |\vec{V}_k-\vec{V}_j| \sigma(|\vec{V}_k-\vec{V}_j|) f(\vec{V}_j) d^3\vec{V}_j\right] \cdot \left.\frac{dt}{dE_f}\right|_{E_f=E_k} \cdot \Delta E \quad (134)$$

where $\Delta E = \dfrac{E_{\ell+1} - E_\ell}{K}$, $E_k = E_\ell + k\Delta E = \dfrac{1}{2} M V_k^2$.

After tedious algebra, it can be shown that if $f(\vec{V})$ is the Maxwellian distribution, then

$$SVB(E_k) \equiv \langle \sigma v \rangle_b \equiv \int |\vec{V}_k-\vec{V}_j| \sigma(|\vec{V}_k-\vec{V}_j|) f(\vec{V}_j) d^3\vec{V}_j$$

$$\equiv \frac{2W_j e^{-u^2}}{\sqrt{\pi}\, u} \int_0^\infty x^2 \exp(-x^2) \sinh(2ux) \sigma(xW_j) dx \quad (135)$$

where $u = V_k/W_j$, $X = |\vec{V}_k - \vec{V}_j|/W_j$, $W_j = \sqrt{\dfrac{2KT_j}{M_j}}$.

It is clear that $\langle \sigma v \rangle_b$ is a function of E_k and T_i. Fortunately, it is relatively insensitive to T_i. We can also define

$$\Delta t(E_k, n_e, T_e) = - \left.\frac{\frac{\Delta E}{dE_f}}{\frac{dt}{dt}}\right|_{E_f = E_k} . \quad (136)$$

This function is very sensitive to E_k, n_e and T_e, but is not sensitive to the ion temperature, or density. Using these expressions, eqn. (134) becomes

$$n_j \sum_{k=1}^{K} SVB(E_k)\, \Delta t(E_k, T_e, n_e) \qquad (137)$$

with $E_k = E_\ell + k\Delta E$, $\Delta E = \frac{E_{\ell+1} - E_\ell}{K}$.

From the preceding discussion, it can be seen that there are three independent quantities to calculate: (1) n_j, which is given by the particle balance equation at each time step; (2) $SVB(E_k)$, which is relatively constant in time and can thus be calculated once for many time steps; and (3) Δt, which has to be calculated in each time step. Since it has been shown that the reaction rate can be considered to be independent of the rate of energy loss, the calculation will be much simpler, and can be done at an acceptable computing cost.

3. Status of Present Wisconsin Advanced Fuel Cycle Burn Kinetics Code

The UW code can handle up to 39 different Maxwellian fast fusion reactions. The code includes: (a) main and control subroutines; (b) subroutines to solve particle balance equations; (c) subroutines which calculate fast fusion probabilities and the slowing down time of fusion products; (d) subroutines to solve the energy balance equations; (e) subroutines to store the results and print out the output; (f) a subroutine to plot the output. In addition a special command has been used to allow fortran statements to be inserted into the code such that one can easily set up the cases for study by following the instructions step by step as stated in the subprogram to change the fortran statements in that subprogram. The special command will then insert the appropriate statements in the proper place in the program.

A block diagram of the code as it exists with the additions to be made is shown in Fig. 13. Among these subroutines, the more important are:

(a) Main and Control Subroutines:

ASVFUL, SETUP, CALCUL, BLOCK, STORE, PRNOUT

(b) Slowing down and fast fusion of subroutine

SLODON, TWOCOM, SIGMVB, GETCS, XSFORM, SXP7LI, XSP6LI, NIROOT.

(c) Particle Balance Equation Subroutines:

CALCU, EQUA, KUTTA, SIGMAV

(d) Energy Balance Equation Subroutines:

FI, BEAMRF, GETSET, PTIEQT, PTEEQT, TIEQTN, TEEQTN

(e) STORAGE AND PRINT OUT SUBROUTINES:

STORE, ELT, PRNOUT, TABLE

(f) PLOTTING SUBROUTINES:

RECPLT, PLOT, SPPLOT

The present version of the code is written in Fortran V and operates on the UNIVAC 1110.

A self consistent steady state version of the code has already been implemented to search for the equilibrium content of the various species in a steady advanced fuel cycle burn. A self consistent method has been derived to calculate the equilibrium contents of p-^{6}Li fuel, p-D-^{6}Li fuel, etc. for various approximate treatments of the p-^{6}Li cycle. The code successfully gives the equilibrium contents of the fuel, calculates the relative power density, neutron production, average neutron energy and so on. We can then search for the self consistent electron temperature, given T_i,

BLOCK DIAGRAM FOR ADVANCED FUEL CYCLE BURN KINETICS CODE

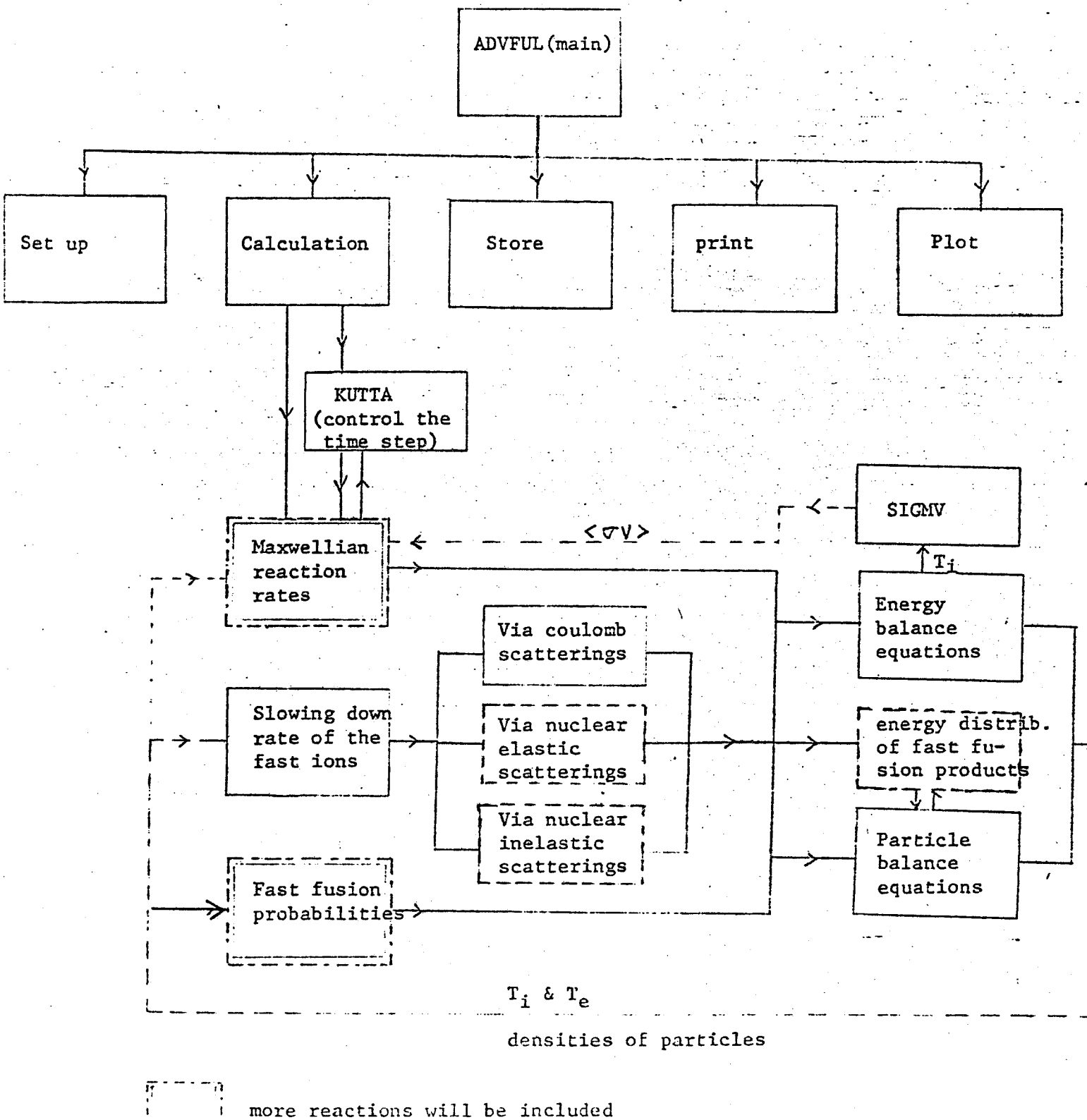

Fig. 13 The Wisconsin Advanced Fuel Cycle Burn Kinetics Code

to determine a solution consistent with electron drag and bremsstrahlung losses to calculate the ratio of fusion power to radiative losses. A number greater than one implies ignition at infinite $n\tau$. We can then determine the energy amplification factor as a function of $n\tau_E$ in equilibrium.

4. Outputs/Summary

The most important outputs of the code are the time history of the density and energy of the various species. The level of radiation losses, charged particle losses, ash removal, as well as the neutron emission (and its spectrum) are also important outputs of the calculation.

The development of this code is now underway at the University of Wisconsin. It is a substantial bookkeeping task in which the reliability of each component calculation must be checked carefully.

When completed, this advanced fuels fusion dynamics code will be a complete, zero dimensional, time-dependent treatment of burn kinetics. It will provide a reasonably inexpensive means of quantitatively evaluating advanced fuel fusion and making a reasonable selection of the most promising confinement concept in which an optimized fuel mixture can be brought to ignition and produce power.

CHAPTER IV

REFERENCES

1. G. H. Miley, et al., Private communication
2. R. D. Sharp and J. Rand McNally,Jr., ORNL-TM-5013, Sept., 1975
3. UCID-17196, Documented by Terry Chu, July, 1976
4. G. Lee, et al., UCRL-74192, Nov., 1972
5. R. Conn and G. Shuy, UWFDM 262, 1978 and private communication

V. Preliminary Results of The Advanced Fusion Fuel Cycle Analysis and Proposed Studies

The effect of propagation and large energy transfer collisions has been shown to be important not only for the catalysed d-d cycle described in chapter I, but also for many other cycles such as p-^{11}B, p-^{6}Li , d-^{3}He , d-^{6}Li.

For the p-^{11}B reaction, the resulting increase in $< \sigma v >$ due to propagating and large energy transfer effects relative to the Maxwellian averaged value is shown in Fig. 14. When this is included in an energy balance calculation, it is found that the p-^{11}B cycle can ignite if the losses are due solely to bremsstrahlung (as opposed to previous studies [1-3] which neglecting these effects showed the maximum Q is less than 3). Using appropriate relativistic formulae for bremsstrahlung and electron-ion rethermalization, the results are summarized in Table 7. Thus, by including propagation and large energy transfer collisions, the prospects for a minimum neutron production cycle have brightened.

Table 7

Power Balance for p-^{11}B Cycle

T_i(keV)	T_e(keV)	$M = \frac{\text{FUSION POWER}}{\text{BREM. POWER}}$	$Q = \frac{\text{FUSION POWER}}{\text{INPUT POWER}}$
200	135	0.83	4.88
250	150	1.00	∞(Ignition)
300	160	1.18	∞(Ignition)

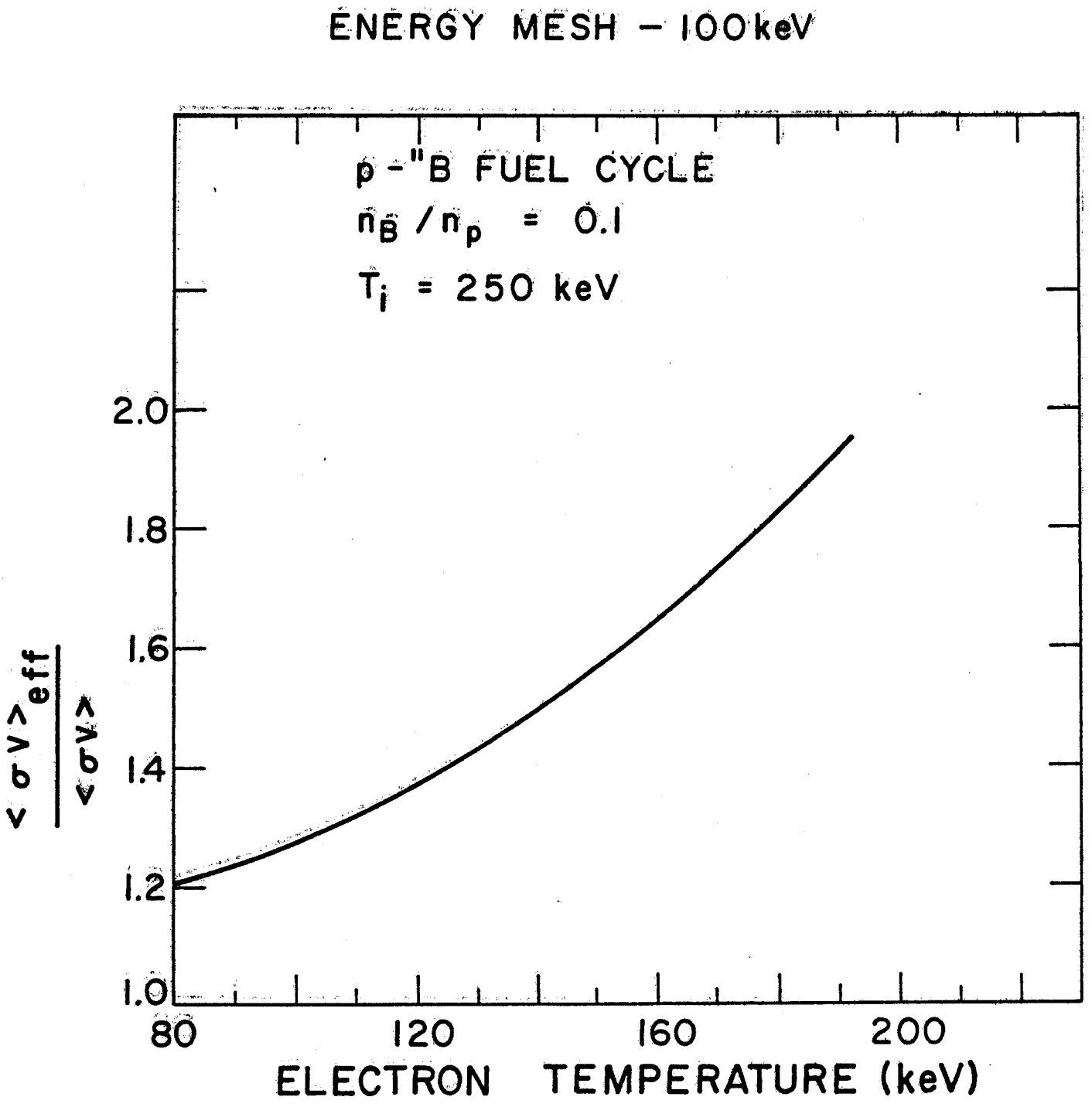
ENERGY MESH – 100keV
p - ^{11}B FUEL CYCLE
n_B / n_p = 0.1
T_i = 250 keV
2.0
1.8
1.6
1.4
1.2
1.0
$\frac{\langle \sigma V \rangle_{eff}}{\langle \sigma V \rangle}$
80
120
160
200
ELECTRON TEMPERATURE (keV)

Fig. 14

Since we have seen, by the previous example, that the effects of propagation and large energy transfer collisions are important, we propose developing a model for advanced fusion fuel cycles which incorporates the relevant physical processes in order to evalute the potential of advanced fuels in future fusion devices. We will

1. Investigate how much these processes affect $n\tau$ requirements for Lawson and ignition conditions or the energy multiplication factor Q, using several models for energy containment time.

2. Utilize the time dependent advanced fusion fuel cycle burn kinetics code to investigate optimum fuel mixture, energy amplification factors, neutron yields, $n\tau_E$ requirements, startup scenarios, ash removal requirements and sensitivity of the burn dynamics to data uncertainty.

References for chapter V

1. J. M. Dawson, UCLA Plasma Group Report, PPG-273 (Aug. 1976)

2. J. G. Cordey, lecture2. Course on theory of Magnetically Confined Plasmas (Varenna, Italy) Sept. 1977

3. R. W. Conn, et al., " Aspects of Octopoles as Advanced Cycle Fusion Reactors " in Fusion Reactor Design Problems, IAEA (Vienna) 1978